AD NUMBER

AD819480

NEW LIMITATION CHANGE

TO

Approved for public release, distribution unlimited

FROM

Distribution authorized to U.S. Gov't. agencies and their contractors; Administrative/Operational use; Apr 1967. Other requests shall be referred to Edgewood Arsenal, Attn: SMUEA-TSTI-T Edgewood Arsenal, MD 21010.

AUTHORITY

USAEA Ltr, 22 Dec 1971

SRI Project PAU-4900

CONDENSATION STUDIES

Special Technical Report No. ..

by

R. C. Robbins
C. Naar

APRIL 1967

DEPARTMENT OF THE ARMY
EDGEWOOD ARSENAL
Research Laboratories
Physical Research Laboratory
Edgewood Arsenal, Maryland 21010

Contract DA-18-035-AMC-122(A)

STANFORD RESEARCH INSTITUTE
Menlo Park, California

DISTRIBUTION STATEMENT

This document is subject to special export controls and each transmittal to foreign governments or foreign nationals may be made only with prior approval of the CO, Edgewood Arsenal, ATTN: SMUEA-TSTI-T, Edgewood Arsenal, Maryland 21010.

DISCLAIMER

The findings in this report are not to be construed as an official Department of the Army position unless so designated by other authorized documents.

DISPOSITION

Destroy this report when no longer needed. Do not return it to the originator.

SRI Project PAU-4900

CONDENSATION STUDIES

Special Technical Report No. 10

by

R. C. Robbins
C. Naar

APRIL 1967

DEPARTMENT OF THE ARMY
EDGEWOOD ARSENAL
Research Laboratories
Physical Research Laboratory
Edgewood Arsenal, Maryland 21010

Contract DA-18-035-AMC-122(A)
Task 1B522301A08101

STANFORD RESEARCH INSTITUTE
Menlo Park, California

FOREWORD

The work described in this report was authorized under Task 1B522301A08101, "Dissemination Investigations of Liquid and Solid (U)." The work was started in July 1965 and completed in January 1967.

The information in this document has not been cleared for release to the general public.

DIGEST

Condensation processes are important in the thermal dissemination of CW agents. Heterogeneous and homogeneous nucleation was studied to determine the important factors controlling condensing systems.

Effects of salt nuclei on the particle size distribution of the disseminated aerosol were studied and special pyrotechnic systems which were salt nuclei-free were investigated.

Aerosols composed of two- to five-micron-diameter particles with a high degree of particle size homogereity make the optimum aerosol for lung retention and maximum transparency. The production of such an aerosol was shown to be feasible by the technique of incorporating non-volatile "giant nuclei" material in the pyrotechnic mix. These giant nuclei when disseminated with the agent vapor acted as preferential condensation sites and as small particle scavengers by coagulation. The secondary process of coagulation was shown to be important in removing the highly visible submicron particles. A pyrotechnic dissemination system was suggested to produce uniform, low visibility aerosols which included coagulation of the small particles to be disseminated on giant nuclei at elevated temperature and high concentrations.

Homogeneous nucleation always occurs in condensing systems of high vapor concentrations even in the presence of foreign nuclei. Critical supersaturation ratios of a number of compounds were measured by a newly developed experimental method. It was demonstrated that the classical Becker-Doering theory is inadequate for the preparation of nucleation models. A modified model is presented showing the interrelationships among physical properties, chemical structure, and temperature.

CONTENTS

ILLUSTRATIONS

1 INTRODUCTION

Pyrotechnic dissemination of liquid or solid agent is accomplished by mixing the agent with the pyrotechnic material. The phase changes in the process include volatilization followed by condensation of the agent. The manner in which condensation occurs establishes the particle size distribution of the disseminated material. If the condensation processes in pyrotechnic dissemination could be isolated and studied separately, then the agent particle size and homogeneity could be controlled.

Condensation involves nucleation, growth, and coagulation (agglomeration). Self-nucleation (homogeneous nucleation) always occurs at some critical supersaturation of a condensable vapor, but foreign nuclei, if they are active, will initiate condensation at lower supersaturation values. The conditions of agent aerosol formation in pyrotechnic dissemination are highly specific, and no theoretical analysis of vapor condensation under these conditions has ever been attempted. The size distribution of the agent aerosol involves the simultaneous kinetics of nucleation, growth, and agglomeration.

Condensation in rapidly quenched jets is dependent on the number and kind of nuclei present. There is considerable experimental evidence that under rapid quench conditions, in the presence of foreign nuclei, homogeneous and heterogeneous nucleation occur simultaneously. Therefore, in order to understand condensation in quenched jets it is necessary to study both heterogeneous and homogeneous nucleation processes. We have made experimental studies of both types of nucleation. These have included (1) an investigation of the aerosol properties of material disseminated from a pyrotechnic device and (2) measurement of the homogeneous nucleation of a number of simple compounds to understand more fully the importance of homogeneous nucleation in actual systems.

II NUCLEATION IN PYROTECHNIC DISSEMINATION

A. Isomorphic Nuclei Effects

The effect of foreign nuclei on the particle size distributions of solid agent simulants vaporized from pyrotechnic devices was studied using a number of different blends of pyrotechnics and agent simulants. These mixtures were burned in unpacked piles and the disseminated simulant was analyzed for size distribution using a six-stage impactor, the Andersen Sampler.† Benzoic acid (BA) phthalic anhydride (PA) and 1-methylaminoanthraquinone (MAA) were the principal simulants used. Potassium chlorate ($KClO_3$) and ammonium picrate (APic) were the oxidizers used.

Inorganic salts (5% by weight) were added to the APic-simulant mixes to provide salt nuclei upon burning. The effect of salt nuclei can be noted in Table I. As in the case of nucleation in condensing jets, large numbers of salt nuclei tend to decrease the particle size and the particle size range of the recondensed material. Also, as observed in the jet nucleation, the salts which are isomorphic appear to produce the greatest effects. The foreign nuclei concentration in these systems is probably critical and may be a quantitative function of nucleation efficiency.

The effectiveness of selected isomorphic nuclei upon condensation is demonstrated by the comparative particle sizes, but the final aerosol properties depend on the relative rates of nucleation, growth from the vapor, and agglomeration of particles already formed. Thus, it would appear to be possible to control size of the particles in a thermal dissemination jet.

† Manufactured by the Andersen Sampler Co., Provo, Utah.

Table I

EFFECT OF COMPOSITION ON MASS MEDIAN DIAMETER OF DISPERSED SIMULANT IN PYROTECHNIC DISSEMINATION

PYROTECHNIC-SIMULANT MIX (wt %)	INORGANIC SALT (5 wt % of Mix)	MASS MEDIAN DIAMETER (microns)
AP_1 (50)/BA(50)	none	2.0
AP1c(50)/BA(50)	KCl	1.0
AP1c(50)/BA(50)	ZnF_2[a]	0.6
AP1c(50)/PA(50)	none	0.8
AP1c(50)/PA(50)	KCl	0.8
AP1c(50)/PA(50)	Na_2CrO_4[b]	0.8[c]
$KClO_3$(50)/BA(50)	none	1.0
$KClO_3$(50)/S(33)/BA(17)	none	1.0
$KClO_3$(50)/S(33)/MAA(17)	none	1.5

[a] ZnF_2 and benzoic acid (BA) are monoclinic.

[b] Na_2CrO_4 and phthalic anhydride (PA) are rhombic.

[c] Narrow size distribution.

B. Thermal Dissemination with Giant Nuclei

The possibility of controlling the particle size of CW agent disseminated by a pyrotechnic device was investigated experimentally. In order to control particle size, giant nuclei were added and mixed into the pyrotechnic-agent blend. The giant nuclei material had to have very definite physical properties:

(1) particle sizes had to be in the 1- to 3-micron-diameter range;

(2) the material could not volatilize appreciably at pyrotechnic burning temperatures; and

(3) the material had to be a preferential nucleator (small interfacial tension with agent).

The materials investigated were silica, magnesium oxide, titanium dioxide, ferric oxide, and alumina.

The pyrotechnic mix could not be a source of effective nuclei. This last condition was the most difficult one to attain. Ammonium picrate, a monopropellant which contains no metal atoms and produces no salt nuclei, was the first fuel-oxidizer used.

The dependence of particle size of condensed organic aerosol particles on the presence of giant nuclei, which were added to the bulk material before vaporization, was demonstrated in a simple nonpyrotechnic volatilization. In an attempt to make a comparative study of the particle size distribution of organic simulants thermally disseminated, with and without selected giant nuclei added to the pyrotechnic mix, a number of mixes were blended and pressed. All mixes contained APic as the monopropellant. The mixes were made with APic (50 and 70% by weight) using benzoic acid, phthalic anhydride, and 1-methylaminoanthraquinone as agent simulants. Additional mixes were made with the same ingredients plus giant nuclei material to the extent of 10% by weight of the simulant. The giant nuclei materials were 1- to 4.5-micron-diameter silica and a pigment grade titanium dioxide. The mixes (i.e., nuclei, propellant, and agent-simulant) were blended in a shaker for several hours and then pressed. A 50:50 mixture of APic and BA and the same mixture plus 5% 1- to 4-micron-diameter silica were fired in separate experiments in a one-cubic-foot meter box. The smoke from each mixture was collected in the Andersen Sampler plus Millipore filter train. The relative amounts of each mixture collected on the backup filters showed that there was several times as much finely divided material from the 50.50 mixture as from the mixture containing silica. However, in both cases there was black smoke, presumably from the inefficient combustion of the APic.

Pyrotechnics based on potassium chlorate will supply large numbers of finely divided (0.1 to 0.01-micron-diameter) KCl nuclei. A second monopropellant which is salt nuclei-free is triaminoguanidine cyanoformate (TAGCY). This compound which was developed at SRI is far superior to APic as an effective monopropellant. TAGCY mixtures containing 1 and 2% APic plus 30% agent simulant were successful pyrotechnics. Ten gram grains of these mixes were pressed at 2000 lb into aluminum film cans of 3 cm in. diameter. Addition of 1- to 4-micron-diameter silica to these pyrotechnic mixes produced a marked increase in the mass median diameter of the disseminated material and a more homogeneous size range. Submicron particles were produced during dissemination, however, and a more efficient scavenging of the smoke was necessary.

Four systems and four coagulation chambers were evaluated for increasing the amount of coagulation in aerosols produced by pyrotechnic means. Changes in relative cloud densities and particle size distributions were the measured parameters. The four chamber designs studied were:

(1) empty cylinder for simple confined coagulations, (2) cylinder with two 8-mesh screens (see Fig. 1), (3) cylinder with two orifice plates, each containing fourteen 1/8-in. holes (see Fig. 2), and (4) a two-stage coagulation device, in which initial coagulation occurs at high temperature and pressure in a confined volume and is followed by simple confined coagulation in a second stage.

All of these coagulation devices were scaled for use with 10 g of pressed mix contained in a 30-mm-diameter canister.

Three types of pyrotechnic mixes were used. The first contained 68% TAGCY, 2% APic, 27% BA, and 3% silicic acid of about 2- to 10-micron-diameter particle size for nucleate seeding. The second and third mixes were based on $KClO_3$-lactose propellant and had different coolant and seeding materials. The second mix was 25% $KClO_3$, 11.5% kaolin, 19.5% lactose, 40% BA, and 4% silica (1- to 4-micron diameter seeding material). The third mix was formulated to check the possibility of using a single additive, silicic acid, for both the cooling and seeding functions. The formulation was 25% $KClO_3$, 19.5% lactose, 44% BA, and 11.5% silicic acid.

Experiments with the TAGCY based mix revealed that screens are more efficient in promoting coagulation than orifice plates and that, even though the velocity through the orifice holes was about five times greater than the velocity through the screen, the dimensions and larger number of turbulent cells caused more coagulation with the screens than with the orifice plates.

The two-stage coagulator showed a greater calculated coagulation rate than the single-stage system. The two-stage approach showed the advantage over the single-stage approach of suppressing homogeneous nucleations in favor of heterogeneous nucleation.

Collision rate calculations follow, based on the kinetic theory of gases and on Smoluchowski's aerosol coagulation theory.[1] The ratio of the calculated collision rates, confined coagulation (two-stage) to unconfined coagulation (single-stage), is about 20:1 in both calculations. The absolute values of the collision rates based on the two theories give rates of the same magnitude.

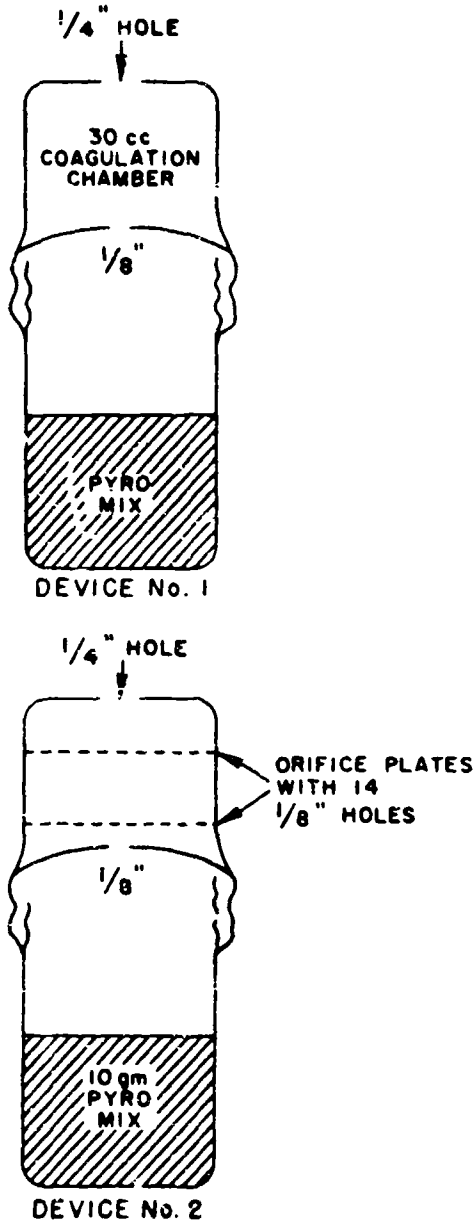

FIG. 2 COAGULATION CHAMBER WITH ORIFICE PLATES

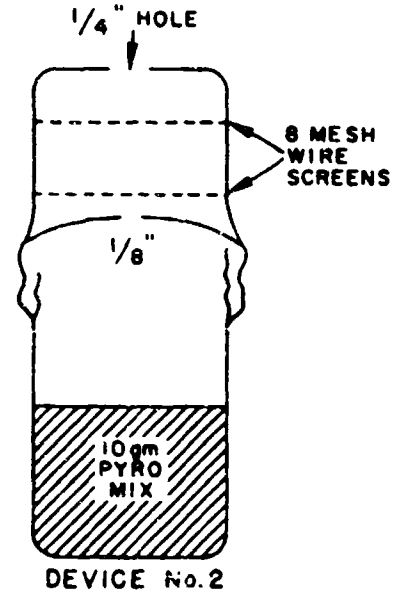

FIG. 1 COAGULATION CHAMBER WITH SCREENS

TA-4900-291

The calculations are based on the following assumptions:

1. For every 10-g charge there is 0.4 g of silica seeding material. Using an average size of 2 microns in diameter, the total number of seeding particles is 5×10^{10}. In the confined coagulation case (2 liters) the concentration is 2.5×10^{7} particles/cc. In the open coagulation case the total volume of gases produced by the 7 g of propellant is calculated to be 8 liters at 300°K for a seeding particle concentration of 6×10^{6} particles/cc.

2. Three grams of BA is about 0.03 mole; this is 1.8×10^{22} molecules, giving a vapor concentration in the confined coagulation case of 10^{19} molecules/cc and a concentration of 2.5×10^{18} molecules/cc in the open coagulation case.

The equation for the collision rate between molecules of two different species in a gas is

$$Z_{AB} = \frac{n_A n_B (\sigma_A + \sigma_B)^2}{4} \left[\frac{8\pi RT(M_A + M_B)}{M_A M_B} \right]^{1/2} , \qquad (1)$$

where

Z_{AB} = number of collisions/sec between molecules A and B

n = number of molecules/cc

$\sigma_{A,B}$ = collision cross section (diameter of molecules A and B)

R = gas constant

T = absolute temperature

M = molecular weight.

If Equation (1) is applied to collisions between vapor molecules and aerosol particles, the effect of any assumed molecular weight for the average aerosol particle is essentially canceled by the form of the expression, i.e., where $M_A \ll M_B$

$$\left(\frac{M_A + M_B}{M_A M_B} \right) \simeq \frac{1}{M_A} . \qquad (2)$$

The calculated values of the collision rates between BA molecules and silica particles are Z_{AB} (confined) = 2×10^{23} collisions/sec at 500°K and Z_{AB} (open) = 10^{22} collisions/sec at 300°K. The Smoluchowski equation expressed as a collision rate is

$$Z_{AB} = K n_A n_B \quad , \tag{3}$$

where K is the coagulation constant. In systems where the aerosol particles are all the same size, K = 3 to 10 $\times 10^{-10}$ cc/sec; in aerosol systems containing two sizes of particles, however, the K for collision between the two sizes increases rapidly with the ratio of the sizes. Fuks[1] has calculated values of K for various size-pairs: the value of K for σ_A - 4×10^{-8} cm (average diameter of BA molecule) and σ_B = 2×10^{-4} cm (average diameter of silica particle) becomes K_{AB} = 2×10^{-4}. The collision rates based on this value of K_{AB} are Z_{AB} (confined) = 5×10^{22} collisions/sec, and Z_{AB} (open) = 3.0×10^{21} collisions/sec.

In open single-stage coagulation the aerosol cloud is rapidly cooled and the critical supersaturation ratio of the disseminated vapor is rapidly exceeded. This produces a large homogeneous nucleation rate, which competes with the condensation on foreign nuclei and produces great numbers of very small (approximately 5×10^{-7} cm) particles. These particles coagulate rapidly to the 2×10^{-5} cm size and become visible as a persistent smoke.

In the two-stage coagulator the minimum temperature is controlled by regulating the pressure during the first several seconds of the burning and vaporization process. By selecting the proper release pressure, a minimum temperature can be reached which will produce a saturation ratio in the confined vapor just exceeding one, thus preventing the occurrence of homogeneous nucleation of the vapor. Also, because of the very low supersaturation value, heterogeneous nucleation on small foreign particles (*i.e.*, carbon nuclei) will be inhibited in favor of heterogeneous nucleation on large foreign particles (*i.e.*, large particles are present in the form of added seeding material).

III HOMOGENEOUS NUCLEATION STUDIES

A. Background

The pressure of a bulk liquid in equilibrium with its vapor is proportional to the absolute temperature T. For an ideal gas, the logarithm of the pressure p is a linear function of $1/T$. It has been observed that in a vapor phase system with no boundaries, condensation will not necessarily occur when the temperature decreases to equilibrium. In the complete absence of foreign droplets, ions or walls the supersaturation reaches an upper limiting value beyond which condensation will always occur. This condensation is called "homogeneous condensation." For a terminal temperature T_f the critical supersaturation ratio is constant and is a function of the nature of the compound. The degree of supersaturation is measured by the saturation ratio S, which is defined as the ratio of the pressure p of the supersaturated vapor at temperature T_f and the pressure p_∞ of the saturated vapor at the same temperature T_f. It has also been observed that the rate of condensation is small until S reaches a critical value after which condensation becomes so rapid that it is impossible to measure the condensation rate directly, for example, by counting the number of drops formed per unit time and per unit volume. The critical value of S at T_f is called the critical supersaturation ratio and is written:

$$S^* = \frac{p}{p_\infty} \quad . \tag{4}$$

Earlier theories of homogeneous condensation related S to the physical characteristics of the compound. These theories were usually based on the experimental observation that "the controlling process in condensation is the *nucleation* of the vapor into droplets." To explain this observation, Gibbs[2] proposed the condition which must exist for nuclei to form in a vapor. Later, the rate of transition from a vapor to liquid phase was studied using classic rate process theory.

1. The Liquid Drop Concept

This concept was originally introduced by Gibbs.[2] He proposed that it is possible to supersaturate a vapor because the formation of a liquid drop requires not only the work needed to transform the vapor into a liquid but also the additional work required to form a stable liquid gas interface. This additional work acts essentially as a barrier of potential in kinetic processes, and it slows down the condensation process. In fact, the free energy of formation of a droplet can be expressed as the sum of two terms: a "bulk" term which corresponds to the free energy of formation of the liquid state from the gaseous phase in the absence of a surface, and a term which is, the free energy formation of the surface.

The free energy difference (per mole) is related to S by

$$\Delta G = RT \ln p_\infty - RT \ln p = -RT \ln S \qquad (5)$$

and becomes negative for $p > p_\infty$.

For a drop of radius r this free energy difference (per drop) is given by

$$\Delta G_1^\circ = -\left(\frac{RT \ln S}{V_0}\right)\left(\frac{4\pi r^3}{3}\right) \quad , \qquad (6)$$

where R is the gas constant and V_0 is the molar volume. The surface term is simply written:

$$\Delta G_2^\circ = 4\pi r^2 \sigma \quad , \qquad (7)$$

where σ is the surface tension.

As the size of the droplet increases, the volume term increases more rapidly than the surface term. Consequently, a critical drop size will be reached after which any increase in radius will cause a decrease of free energy, and therefore spontaneous condensation will occur. It is in the above sense that the surface properties act as a barrier of potential. The total free energy of formation of one condensing droplet is then

$$\Delta G^\circ = -\left(\frac{RT}{V_0}\right)\left(\frac{4\pi r^3}{3}\right) \ln S + 4\pi r^2 \sigma \qquad (8)$$

and is maximum for a critical value r^* of r such that

$$\Delta G^* = \frac{16\pi\sigma^3}{3\Delta G^2} \tag{9}$$

and

$$r^* = \frac{2\sigma}{\Delta G} \quad . \tag{10}$$

This value ΔG^* is thus the barrier which must be exceeded for homogeneous nucleation to occur. These critical size droplets, also called nuclei or clusters, are present in supersaturated vapors, even if no phase transition occurs. Note that Equation (7) is the well-known Gibbs-Thomson relationship.

As already mentioned above, Gibbs[2] established on a firm basis the equilibrium conditions that must exist for nuclei to form in a vapor, but he did not study the conditions for transition from a supersaturated vapor with a few nuclei to a condensed vapor with a very large number of drops. The adaptation of rate process theories to the problem of homogeneous nucleation was the next step in understanding this phenomenon. This is described in the next section.

2. The Transition Process

The first attempt to describe the nucleation rate J was made by Volmer and Weber.[3] They proposed that J be taken as a product of two terms—an energetic and a kinetic term. The energetic term n_i^*, defined as the concentration of nuclei in the vapor, can be related to ΔG^* by

$$n_i^* = n_1 e^{-\Delta G^*/kT} \quad , \tag{11}$$

where n_1 is the number of molecules/cm^3 (this establishes an equilibrium state between clusters of different size). The kinetic term w is the frequency of collision of nuclei per surface unit $4\pi r^{*2}$ and can be deduced from the kinetic theory of gases:

$$w = \frac{p}{(2\pi m k T)^{1/2}} \quad , \tag{12}$$

where p is the supersaturated vapor pressure and m is the mass of the nuclei. Hence, the Volmer-Weber equation for the rate of nucleation is:

$$J = n_1(4\pi r^{*2})\left(\frac{p}{\sqrt{2\pi mkT}}\right)e^{-\Delta G^*/kT} \quad . \tag{13}$$

It follows therefore that n_1 can be related to the supersaturation vapor p in the case where the vapor is considered as a perfect gas:

$$n_1 = \frac{p}{kT} \tag{14}$$

and that ΔG^* is related to S^* (compare Equations (5) and (9). Because the rate of condensation becomes very rapid when S reaches S^*, it is not possible to measure J. Consequently, the theory assumes instead that when one drop is formed per cc per second ($J = 1$), S has reached its critical value, and for this condition a theoretical value of S^* is calculated and can be compared with the experimental value of S.

Other theories have been proposed which differ from Volmer and Weber's[3] initial formulation. These theories differ mainly in the expression of one or both of the two terms—kinetic and energetic. Volmer and Weber's theory was refined by multiplying the frequency term by a condensation coefficient ($\alpha_c \leq 1$) to account for collision efficiencies (α_c is usually taken to equal one).

Becker and Doering[4] refined the energetic term by taking the steady state instead of the equilibrium state to calculate the concentration of nuclei in the vapor. They considered the set of bimolecular reactions

$$A_1 + A_1 \rightleftharpoons A_2 \tag{15}$$

$$A_2 + A_1 \rightleftharpoons A_3 \tag{16}$$

$$\vdots \qquad\qquad \vdots$$

$$A_{i-1} + A_1 \rightleftharpoons A_i^* \tag{17}$$

where A_i^* is the critical nucleus containing i molecules. The concentration n_i^* is then calculated for this steady state and is written in the form

$$n^* = Zn_1 e^{-\Delta G^*/kT} \quad . \tag{18}$$

Here Z, usually called the nonequilibrium factor, is given by

$$Z = \left[\frac{\Delta G^*}{3\pi kT i^{*2}}\right]^{1/2} \tag{19}$$

where i^* is the number of molecules in the critical nuclei. The Becker-Doering equation for nucleation rate is then written in the form

$$J = (\alpha_c 4\pi r^{*2}) Z \frac{p}{(2\pi mkT)^{1/2}} n_1 e^{-\Delta G^*/kT} \quad . \tag{20}$$

When $J = 1$ and $\alpha_c = 1$, the equation can be written in the form,

$$2(\ln S^*)^3 + b(\ln S^*)^2 - a = 0 \quad , \tag{21}$$

where a and b are functions of density d, surface tension σ, vapor pressure p_∞, and molecular weight M, for any specific temperature T_f.

$$a = 17.557 \frac{\sigma^3}{T_f^3}\left(\frac{M}{d}\right)^2 \tag{22}$$

$$b = 45.435 + \ln\left[\frac{(M\sigma)^{1/2}}{d}\left(\frac{p_\infty}{T}\right)^2\right] \quad . \tag{23}$$

The size of the critical cluster is then:

$$i^* = \frac{2a}{(\ln S^*)^3} \quad . \tag{24}$$

More recently, Lothe and Pound[6] proposed that the free energy of formation ΔG^* should be corrected by a term $\Delta G_1^{*\prime}$ to account for the motion of the droplet as a whole (ΔG^* being computed for a critical cluster at rest). This term can be calculated from the rotational and transitional partition functions of the cluster. Lothe and Pound included another correction term $\Delta G_2^{*\prime}$ arising from the requirement of conservation of the degrees of freedom of the cluster from the vapor phase to the liquid phase. This term[6] has been shown to be approximately equal to Ts, where s

is the molecular entropy of the liquid. The rate of nucleation after correction is then written in the form:

$$J = \alpha_c Z \Gamma (4\pi r^{*2}) \frac{p}{(2\pi m k T)^{1/2}} n_1 e^{-\Delta G^*/kT} \quad , \tag{25}$$

where $\Gamma = e^{-\Delta G^{*\prime}/kT}$ is the Lothe-Pound factor. An error of 4π was found in checking the derivation of this equation; the corrected equation is:

$$\Gamma = (IkT)^{3/2} \frac{kT}{p} \frac{i^*}{\pi^2} \frac{(2\pi m k T)^{3/2} e^{-\varepsilon/k}}{4\pi \hbar^6} \tag{26}$$

which reduces to

$$\Gamma = \frac{(mI)^{3/2} (kT)^4 i^{*3/2} e^{-\varepsilon/k}}{\pi p \hbar^6} \quad . \tag{27}$$

Here $\hbar$ is the Planck constant h divided by 2π, and I is the kinetic moment of the critical cluster, equal for a spherical droplet to

$$I = \frac{2}{5} m i^* r^{*2} = \frac{2}{5} i^* \frac{M}{N} r^{*2} \quad . \tag{28}$$

Taking $J = 1$ and $\alpha_c = 1$, we have utilized the Lothe-Pound equation [see Equation (25)] σ_0 as a function of d, σ, p_∞, and S^*, introducing a new function λ independent of S^*, such that

$$n\Gamma = \lambda - \ln S^* - 12 \ln (\ln S^*) \quad , \tag{29}$$

where

$$\lambda = \ln \frac{24\sqrt{2}}{5^{3/2} \pi^2 N^4} \frac{k^4}{\hbar^6}$$

$$= \ln \frac{k^4}{\hbar^6} + 4 \ln a - \frac{S}{Nk} - \ln p_\infty d + 4 \ln MT \quad ,$$

$$= 6.21132 + 4 \ln a - \frac{S}{R} - \ln p_\infty d + 4 \ln MT \tag{30}$$

and $X = \ln S^*$ yields

$$X^3 + X^2\left\{b + \lambda - \frac{1}{2}\ln a - 12\ln X + \frac{1}{2}\ln\left[a + X^3 + X^2(12\ln X - \lambda)\right]\right\} - a = 0 \quad . \qquad (31)$$

This simplified form of Equation (25) is equivalent to the Lothe-Pound nucleation rate equation. Solving this equation for specific values of a, b, and λ, we obtain from the root $X = \ln S^*$ the theoretical value of the critical supersaturation ratio, which will be compared to the measured values of S^*. i^* may be calculated by

$$i^* = \frac{2a}{X^3} \quad . \qquad (32)$$

To measure the critical supersaturation ratio, the following techniques have been used: the expansion chamber technique, the diffusion technique, and the jet technique. The basis of these techniques is to cool the vapor very rapidly by enforcing sudden changes of temperature. It is hoped that in this way the vapor will become supersaturated before it can diffuse and condense on the wall of the measuring container or chamber.

a. Expansion Chamber Technique

The measurements of Wilson and Powell,[8] using expansion chamber techniques, give consistently high values for the critical supersaturation ratios of water. The expansion chamber technique consists of cooling the vapor by suddenly expanding a mixture of the vapor with an inert carrier gas. If the expansion is assumed to be adiabatic and reversible, the final temperature can be computed from the ratio of the volumes before and after expansion, from the initial temperature, and from the heat capacities at constant pressure and constant volume, respectively. Unfortunately, under conditions of reversibility and adiabacity, the expansion ratio cannot be higher than 1.3 or 1.4. This limits the range of temperature that can be investigated and if the critical supersaturation ratio is too large (as in the case for CCl_4, for example) it may be impossible to measure S^* by this technique. Wilson and Powell[8] measured the critical supersaturation ratio of water for temperatures ranging from 260 to 325°K. Critical supersaturation ratios of some organic compounds, such as nitromethane, ethylacetate, and a few alcohols, have been measured by Volmer and Flood.[9]

Clarke and Rodehush[10] measured S^* for water and benzene using helium as a carrier gas. Their reported values of S^* are small—probably because of heterogeneous condensation.

b. Diffusion Technique and Measurements

Recently Katz and Ostermier[11] have used this technique for measuring critical supersaturation ratios. Their results are in agreement with those of Volmer and Flood.[9] The diffusion technique was originally used to determine only the S^* for solidification of a supercooled liquid. This technique, which uses the actual steady-state condition during the measurement, appears to be very promising for obtaining critical supersaturation ratios. Unfortunately, it is also limited to a small temperature range, and it requires the knowledge of the transport coefficients.

c. The Jet Technique

This technique has been used by Higuchi and O'Konski.[12] It is a valuable approach to critical supersaturation measurement but it can be used only for compounds of low volatility because of experimental limitations.

3. Discussion of Comparative Data

The critical supersaturation ratios measured by Volmer and Flood[9] for organic compounds are found to be in excellent agreement with the values predicted by the Becker-Doering equation. The Wilson-Powell measurements for water were also in a relatively good agreement at high temperatures.

It was not until recently, when Lothe and Pound[6] suggested their correction to the Becker-Doering theory (a correction that increases the nucleation predicted by the Becker-Doering equation by a factor of 10^{17}), that a possible means of reconciling Becker-Doering theory with experiment was seriously attempted.

In view of these discrepancies it became important to plan further experimental investigations to determine whether the correction proposed by Lothe and Pound was necessary. For example, it appeared desirable to measure S^* for water over a larger temperature range. In the course of our condensation studies, we developed a method of measuring S^* over very large temperature ranges. This development and the S^* data acquired will be described in the following sections.

B. Experimental Studies

In devising a new technique for measuring S^* a flow method was chosen, which was similar to the Y-flow method used in gas kinetics to study reaction rates. The Y-flow method has been described by Bodenstein and Wolgast,[13] Langmuir,[14] and Benton.[15]

1. Description of the New Apparatus

Instead of mixing the flows arriving from the branches of the Y, it was decided to have the gases arrive head-on at the mixing zone. The basic principle of the apparatus is simple. A hot gas stream, saturated with the vapor of interest, is made to collide head-on with another gas stream which is much colder. The two streams come together in a small chamber; the mixing region between the tube ends is centered in the path of a strong, collimated light beam which is placed at such an angle as to produce forward scattering of maximum intensity from any droplets which might be formed. The cold stream temperature is controlled by passing the diluent stream through a massive cylindrical copper thermostat submerged in a cooling bath. The hot copper thermostat, which is heated with electric heating tape, is placed directly over the cold one and the two are mutually insulated by 3/4-in. cork. The hot copper thermostat is also an isothermal vaporizer. The liquid of interest is placed in a well in the hot cylinder. A measured flow of nuclei-free, dry air is passed into the thermostated liquid through a fritted glass bubbler. The gas, vapor, and entrained droplets then pass through two layers of Gelman Type A glass fiber filter to remove all of the liquid droplets and to assure saturation of the gas stream. The gas-saturated vapor stream is then passed through a deionizer in the form of a small annular condenser. The copper inlet line to the cold thermostat has a similar condenser. The distance between the surfaces in these condensers is 1 mm and they are about 5 cm long. A 45-volt field is used for gas-ion removal. Figure 3 shows a detailed schematic of the apparatus.

2. Technique Description

Both the hot and the cold flows must be limited to laminar flows. This provides for steady-state conditions in the mixing region, isolated from any wall effects, as shown in Fig. 4. Since stream temperatures, pressures, and composition are known, only the heat capacities of the

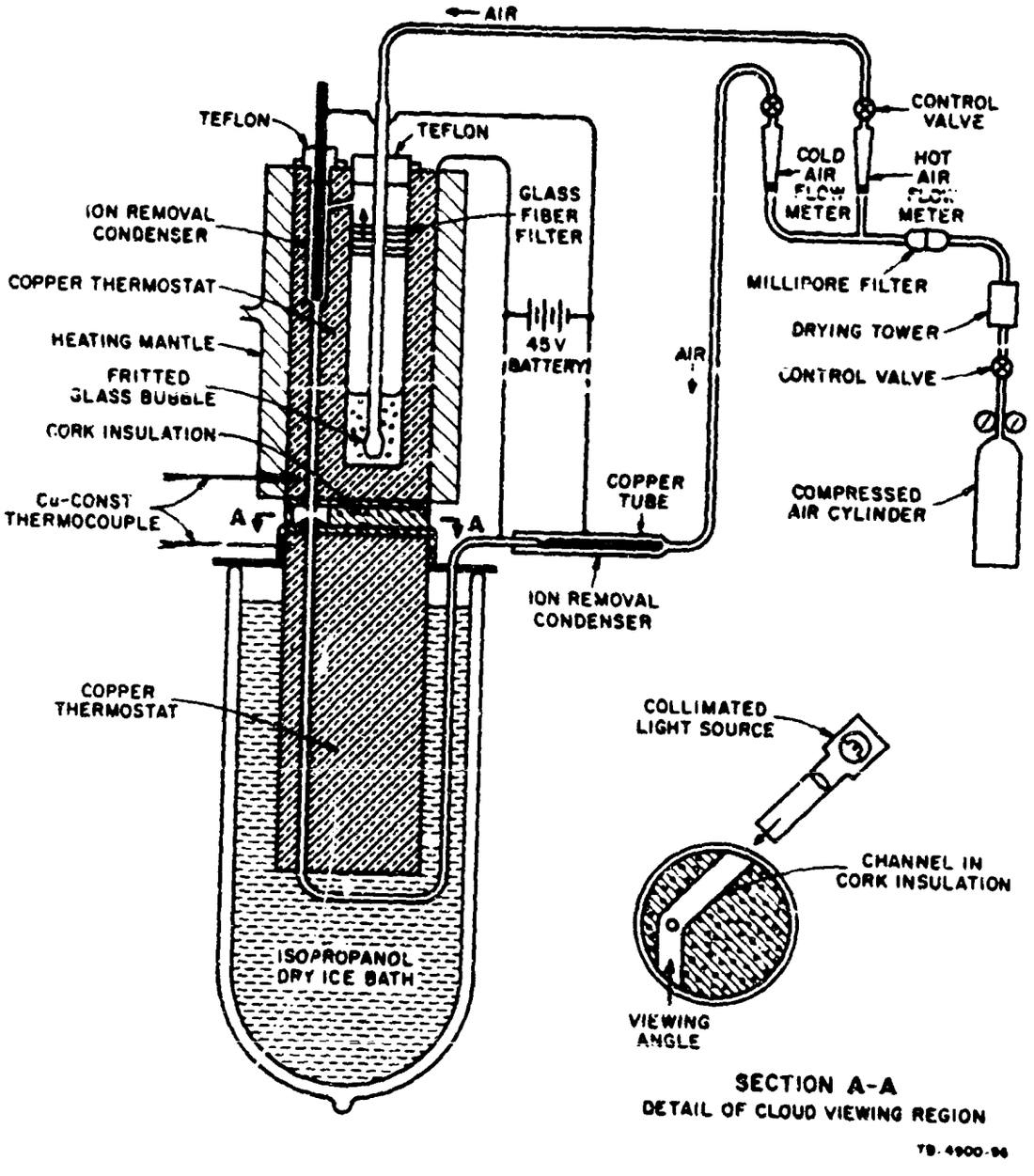

FIG. 3 APPARATUS FOR MEASURING HOMOGENEOUS CRITICAL SUPERSATURATION RATIOS

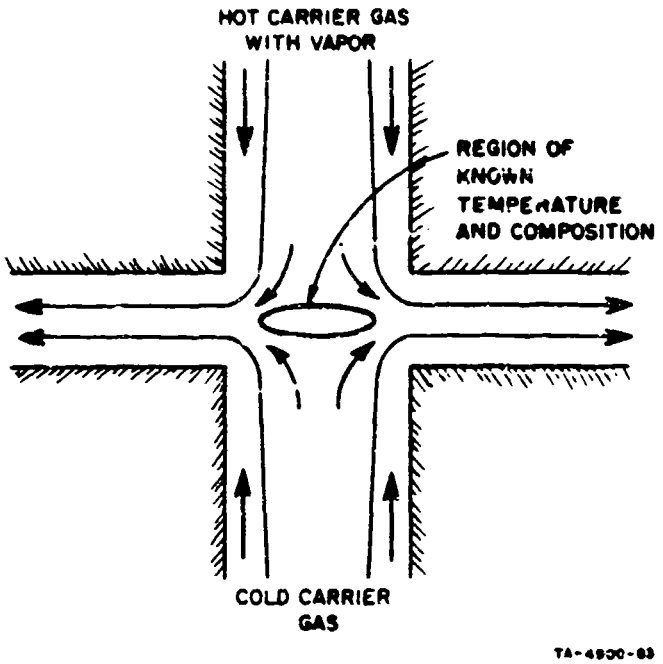

FIG. 4 STEADY-STATE MIXING REGION

gaseous components need to be determined to calculate the temperature of the mixing region. One of the flow rates or one of the temperatures is adjusted to initiate nucleation, which is detected by observing the forward scattered light. The temperature of the mixing region (T_f) is completely controlled by the mixing processes. The heat of condensation is much too small to change the stream temperatures which are measured by means of thermocouples in the copper thermostats very close to the tube exits.

To calculate the mixing temperature T_f, the total heat gain of the cold stream ΔQ_c is set equal to the total heat loss of the warm stream ΔQ_w; i.e.,

$$\Delta Q_c = \Delta Q_w \quad , \tag{33}$$

$$\Delta Q_c = F_c C_p (T_f - T_c) \quad , \tag{34}$$

$$\Delta Q_w \quad \left[F_w C_p + F_w \left(\frac{p}{760 - p} \right) C_{p(v)} \right] (T_w - T_f) \quad , \tag{35}$$

where C_p is the average heat capacity of the air, $C_{p(v)}$ is the average heat capacity of the compound vapor, F_c and F_w are the cold and warm stream flow rates, and T_c and T_w are the cold and warm stream temperatures. By combining Equations (34) and (35), T_f can be calculated. When T_f is established S^* is easily calculated:

$$S^* = \frac{(\text{measured } p \text{ at } T_f)}{(\text{saturated } p_\infty \text{ at } T_f)} , \tag{36}$$

where the measured vapor pressure in mm Hg at T_f is

$$p = \left(\frac{F_w \frac{p'}{760 - p'}}{F_c + F_w + F_w \frac{p'}{760 - p'}} \right) 760 \tag{37}$$

where p' is the saturated vapor pressure at T_w and p_∞ at T_f is deduced from the curve for saturated vapor pressure versus $1/T$ for the pure compound.

To gain a better understanding of the capabilities and limitations of the technique, it appeared desirable to study the variation of S^* with the ratio of temperature T_w/T_c or the ratio of flow rate F_w/F_c of the gases being mixed. From Equations (33) - (37), we can deduce S and T_f, and we notice that if T_c and T_w are kept constant, S will vary with the ratio F_c/F_w. There is a maximum value for S that will correspond to a specific value of F_c/F_w and, since T_c and T_w are kept constant, to a specific final temperature T_f. Figure 5 shows a curve of S versus $1/T$ for CCl_4 at $T_c = 175°K$ and $T_w = 300°K$. Curves (such as the one in Fig. 5) can be used to visualize how S could vary to reach the observed critical values, and to choose the appropriate values for T_c and T_w for a specific experiment. Thus, it can be seen that S will reach this critical value by varying F_c/F_w and keeping T_c and T_w constant (see Fig. 5).

The interrelationships between accuracy, S^*, and the F_c/F_w ratio were quite complicated because of the physical characteristics of the system. The S^* is easy to measure when an initially large F_c/F_w ratio is decreased slowly to the onset of condensation. The drawback to this approach is that S^* occurs at large F_c/F_w ratios (*cf.*, $F_c/F_w = 70$ in

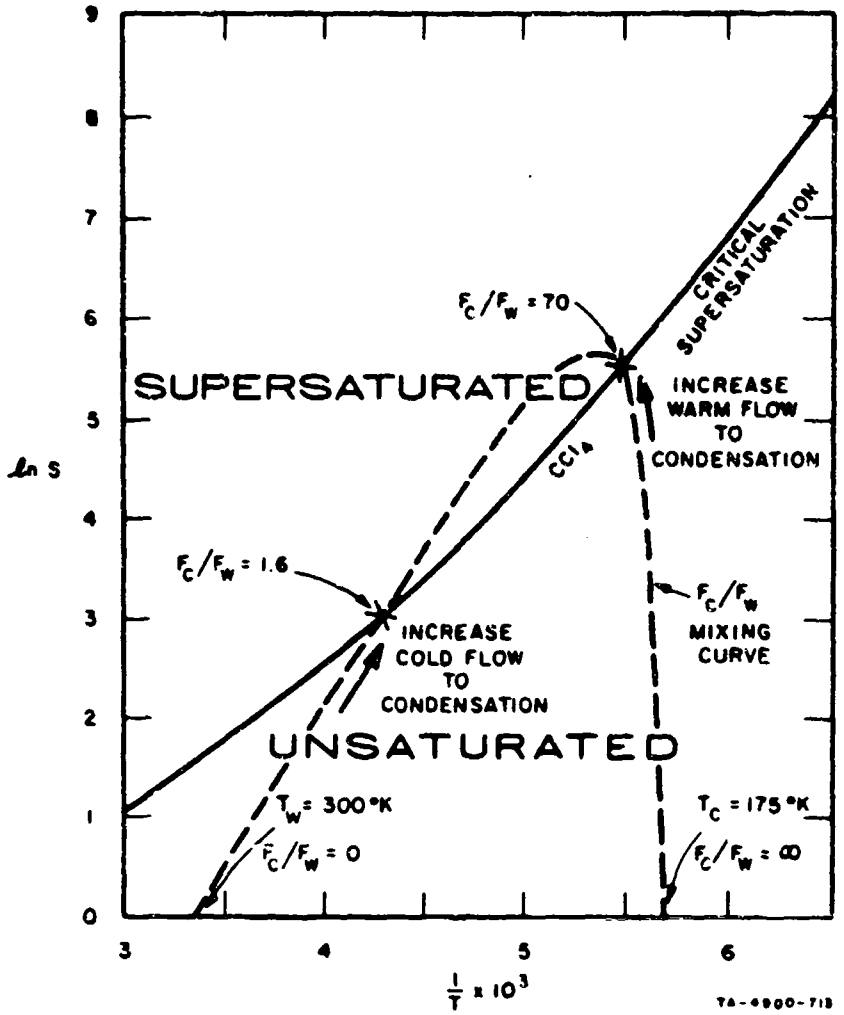

FIG. 5 EXAMPLE OF LIMITS OF COLD AND WARM FLOW RATIOS IN THE MIXING STREAMS TECHNIQUE

Fig. 5); under these conditions, the mixing region is displaced toward the warm air outlet, and this may affect the observed condition for the onset of condensation. When S^* is approached from the other direction, *i.e.*, when an initially small F_c/F_w ratio is increased slowly to the onset of condensation, the value of the F_c/F_w ratio is close to one (*cf.*, $F_c/F_w = 1.6$ in Fig. 5), and the mixing region is not displaced. However, large amounts of condensate form on the viewing chamber surfaces and cause difficulties. We have been making measurements using the initially small, increasing F_c/F_w approach for comparative purposes.

In measuring critical supersaturation ratios when $F_c = F_w$, a large temperature difference between the two air flows is necessary. We found that for $F_c = F_w$, the final temperature range is limited to a practical interval of about 60°K (192 to 253°K in the case of CCl_4). Thus it remains necessary to accept the experimental difficulties accompanying the large F_c/F_w ratio approach in order to conveniently measure S^* at temperatures outside this temperature range.

Because of the relatively small dimensions of the mixing zone, it is necessary to determine whether or not the residence time of the mixing gas and vapor was adequate to establish steady-state conditions of cluster and embryo populations. The induction period (time required to form clusters and embryos) at critical supersaturation is estimated to be about 10^{-7} sec. At a total air flow of 2 liters/min., the gas in the mixing zone travels about 5×10^{-5} cm in 10^{-7} sec. Since the minimum dimension of the mixing is its thickness, estimated to be about 10^{-3} cm, the residence time is more than adequate to establish steady-state conditions.

Finally, an analysis was made of the effect of both total air flow and the ratio of the cold air flow to the warm air flow on the accuracy of critical supersaturation ratio measurements.

The optimum total air flow should be between 1 and 2 liters/min. Flows which are too small cause errors in measurement of the temperature. Flows greater than 2 liters/min produce turbulence in both the cold and warm air streams and could cause distortion of the mixing zone.

Using this technique S^* values were measured for benzene, CCl_4, CS_2, $CHCl_3$, and H_2O. It was possible to obtain very high values for S^* for a range of temperature much larger than any range that had been investigated in previous studies.

3. Potential Sources of Errors and Description of the Second and Third Generation Apparatus

As measurements progressed, it was possible to gain a better understanding of potential sources of errors in the new technique. These potential errors, together with the corrective steps that were adopted to improve the apparatus, are discussed below.

A possible source of error in the very cool temperature experiments could have been created by water from the ambient wet air diffusing into the mixing chamber and condensing. To eliminate this possibility the apparatus was modified to isolate the condensation chamber. This change eliminated the possibility of partial obscuration of the condensation zone by external moisture condensation. The modified apparatus is shown in Fig. 6. The first condensing droplets were much easier to detect than they had been previously, and the accuracy of the apparatus was improved considerably.

The arrival of the dry air directly, without its being brought to the equilibrium temperature of the upper thermostat, created problems in measuring S^* of compounds with low or high vapor pressure, since the temperature of the upper thermostat was quite different from room temperature. To eliminate this limitation, a new vapor saturated-warm air thermostat apparatus was designed and fabricated. The general features were the same as in the first apparatus, but the gas preheating, the thermostating, and the filtering were improved. Figure 7 shows the new parts in detail. The air flow temperature can reach the thermostat temperature or the equilibrium temperature of the saturated vapor before it mixes with the liquid to carry the vapor. In Fig. 7 the air is preheated at the cylinder temperature by circulating it in a copper pipe around the copper cylinder. Then it goes into the vaporization chamber to carry the saturated vapor through the glass tube and the fritted glass bubbler. In the first prototype the air was channeled directly to the glass tube.

We have also made some measurements using two warm sections of the apparatus, set up in series. The first warm section was used as a vaporizer, producing saturated vapor at temperature T_v. The second warm section, into which the saturated vapor was introduced, was used as a thermostated superheater. This arrangement provides a simple way to clear the viewing chamber of condensate. This can be done by circulating dry, clean air in the system before admitting the vapor to the apparatus.

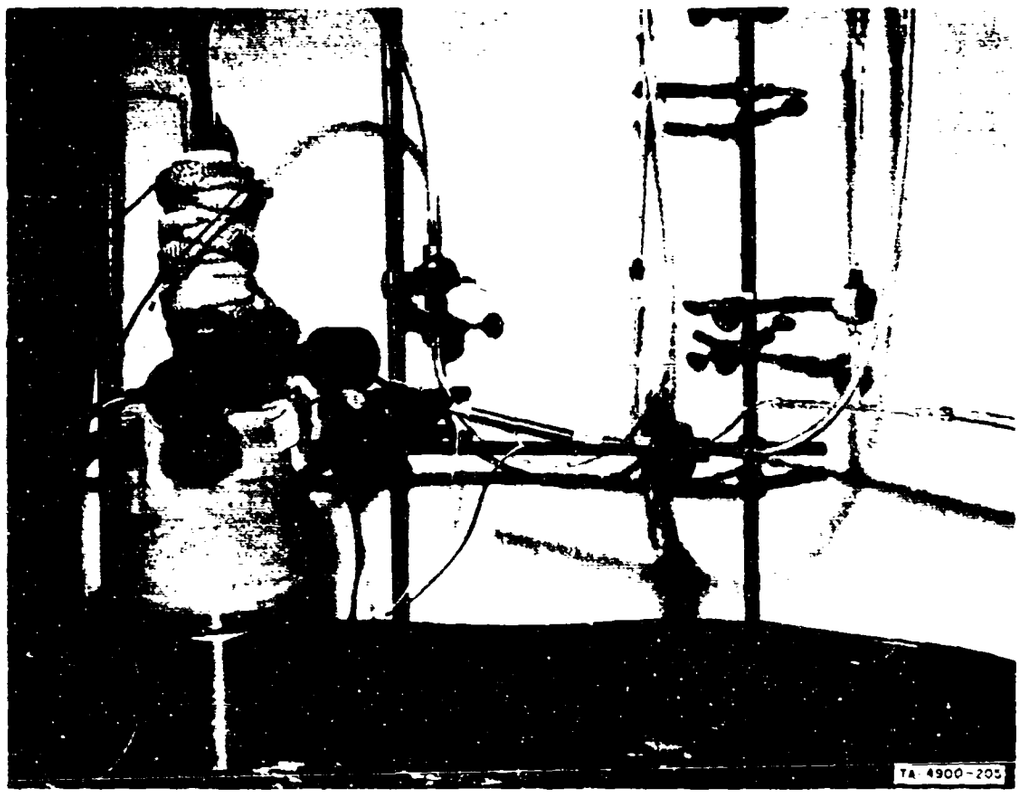

FIG. 6 THE CRITICAL SUPERSATURATION RATIO MEASUREMENT APPARATUS

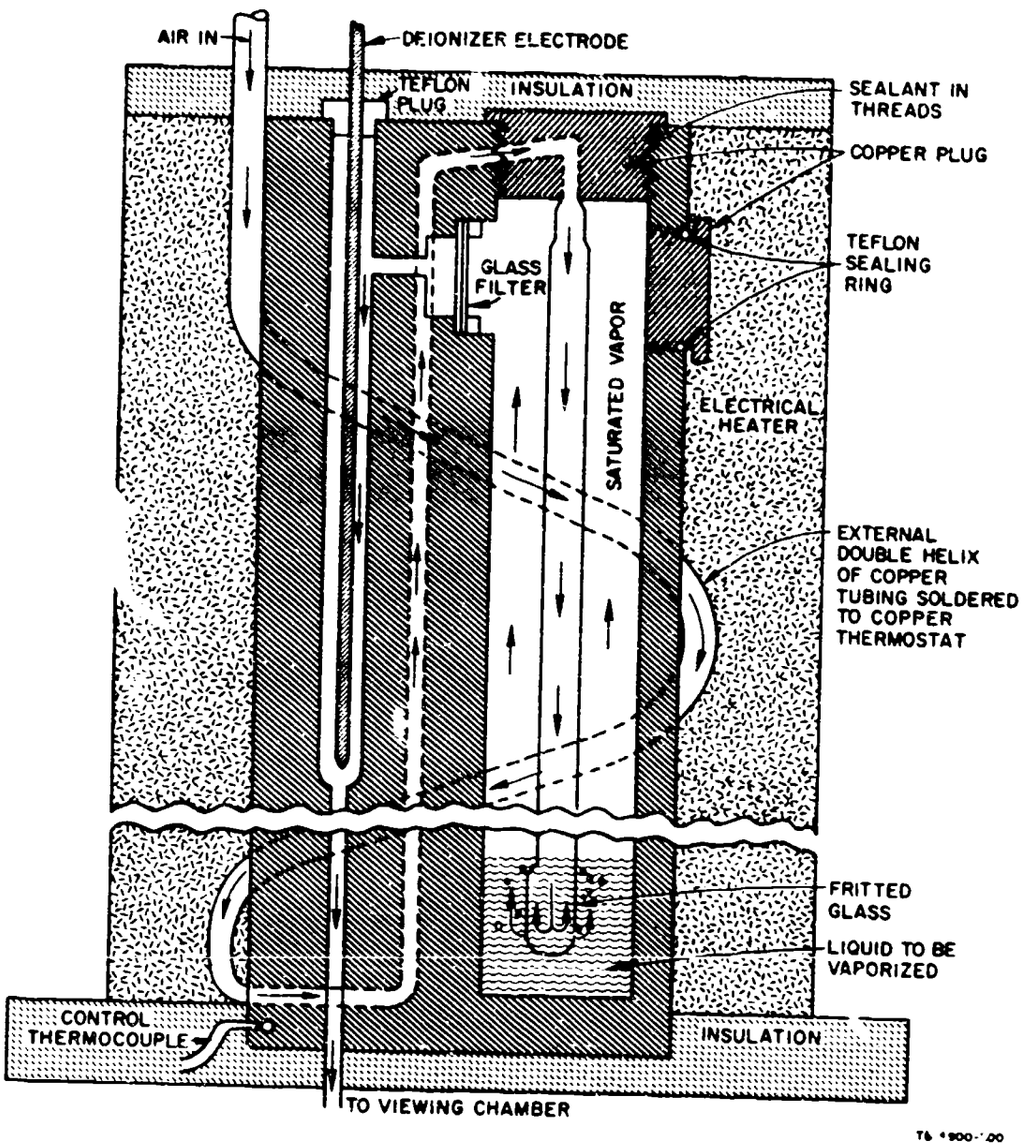

FIG. 7 MODIFIED WARM THERMOSTAT-VAPORIZER SECTION OF CRITICAL SUPERSATURATION MEASUREMENT APPARATUS

C. Experimental Results

Curves of $\ln S^*$ versus $1/T$ were constructed for several simple compounds over wide temperature ranges.

1. Water

The critical supersaturation data for water vapor from a previous study[16] and from the present work are summarized in Fig. 8. A comparison of our results with the results of others shows that there is agreement between our measurements and those of Wilson and Powell,[8] whose results have been considered the best available.

Sander and Damkoehler[17] and Madonna *et al.*,[18] claimed to have observed freezing nucleation of water at low temperatures (homogeneous condensation from the vapor phase to the solid state). We have not observed scintillations upon condensation and construe this to mean that the condensed particles were liquid. As the temperature decreased, the size of the nuclei kept getting smaller, and the aspect of the cloud kept changing gradually from droplets to smoke. The temperature, -65°C is generally believed to be a transition temperature, below which water must crystallize

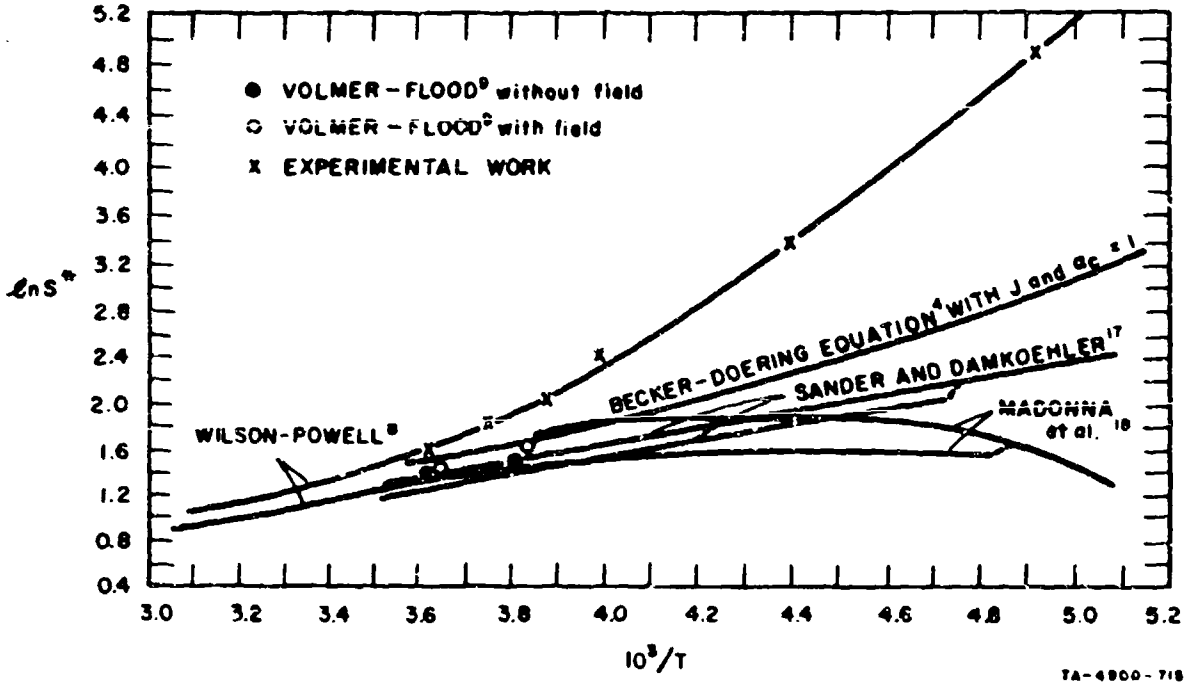

FIG. 8 COMPARATIVE CRITICAL SUPERSATURATION CURVES FOR WATER VAPOR

when condensing. Hirth and Pound[16] take -41°C as this lower temperature limit because -41°C is the critical temperature for rapid homogeneous nucleation of ice from supercooled water, but our observations lead us to believe that nucleation occurs from the vapor to the liquid state at temperatures lower than -65°C.

2. Organic Compounds

Figures 9-12 show curves of $ln\ S^*$ versus $1/T$ for benzene, carbon tetrachloride, carbon disulfide, and chloroform. Computations from the experimental data were done with the TWX Time Share Computer system.

Results of an error analysis showed that both saturated vapor pressure and temperature had been measured with a high degree of accuracy and that largest errors were probably caused by promoters of nucleation such as foreign nuclei. Nevertheless, we did find some systematic error in a small range of temperature, and we investigated the possibility that it might have resulted from a temperature gradient in the cold thermostat when liquid nitrogen was used as cooling bath. Because the error was systematic we were able to correct the measured T_c (when the liquid nitrogen level was beneath the copper thermostat a maximum correction of -20°K had to be applied).

For benzene we were able to make a very difficult measurement at relatively high temperature T = 270°K for F_c equal to F_w approximately and found S^* = 8.0. We obtained a slower rate of nucleation than Clarke and Hodel sh,[10] who found S^* = 8 at 250°K. This result indicates that they may have h heterogeneous condensation when they measured S^* for benzene. They e using helium as a carrier gas.

D. Discussion and Conclusions

1. Comparison of Experimental Results with Earlier Theories

Figures 9-13 show the curves of $ln\ S^*$ as a function of the inverse of the absolute temperature $1/T$ for water, benzene, carbon tetrachloride, carbon disulfide, and chloroform. To calculate the theoretical critical supersaturation ratio for these compounds, we have extrapolated the liquid-state physical properties to very low temperatures. The experimental data appearing in the theoretical expressions are the density,

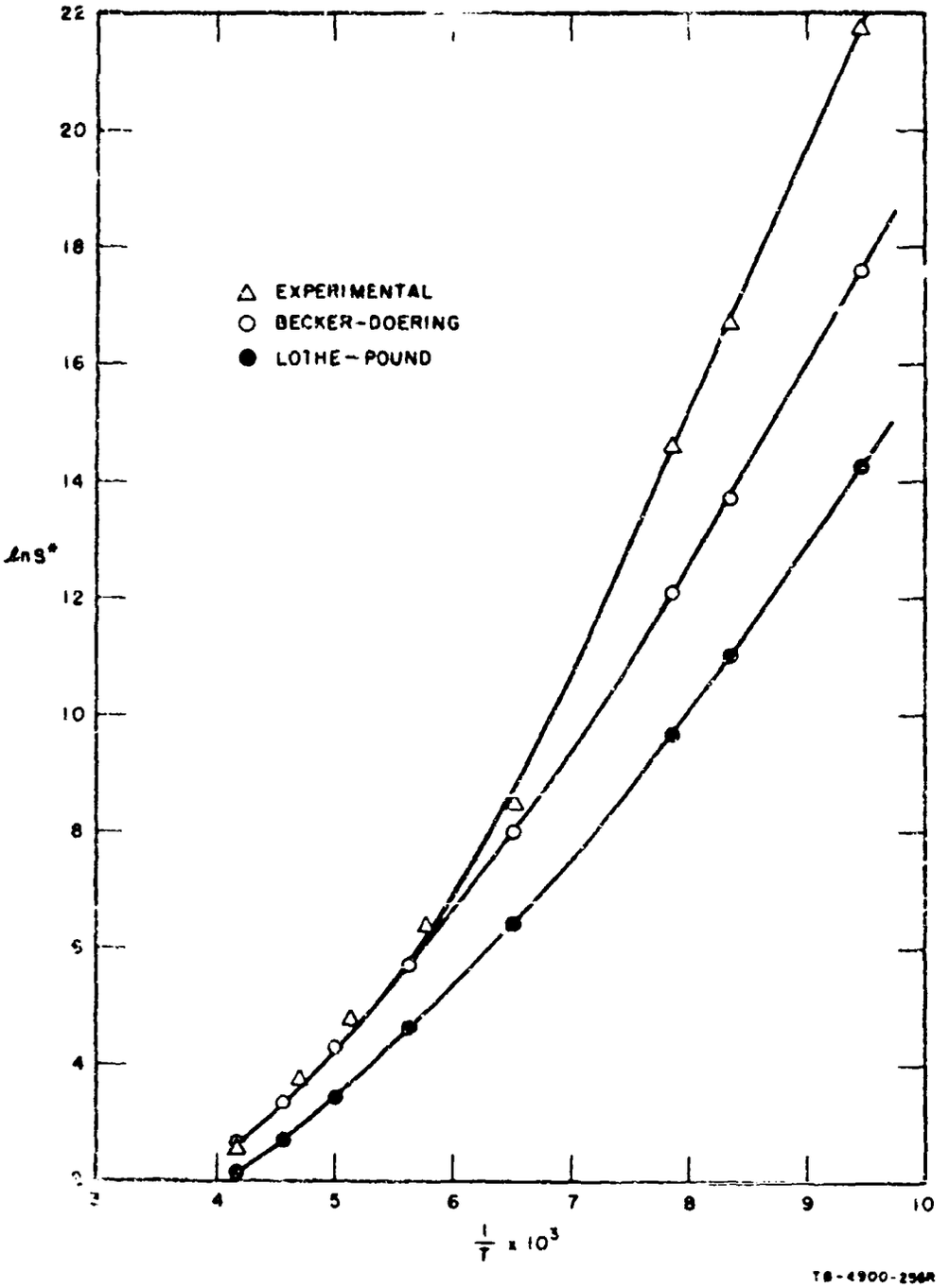

FIG. 9 LOGARITHM OF SUPERSATURATION RATIO AS A FUNCTION OF THE INVERSE OF THE ABSOLUTE TEMPERATURE FOR HOMOGENEOUS NUCLEATION OF BENZENE

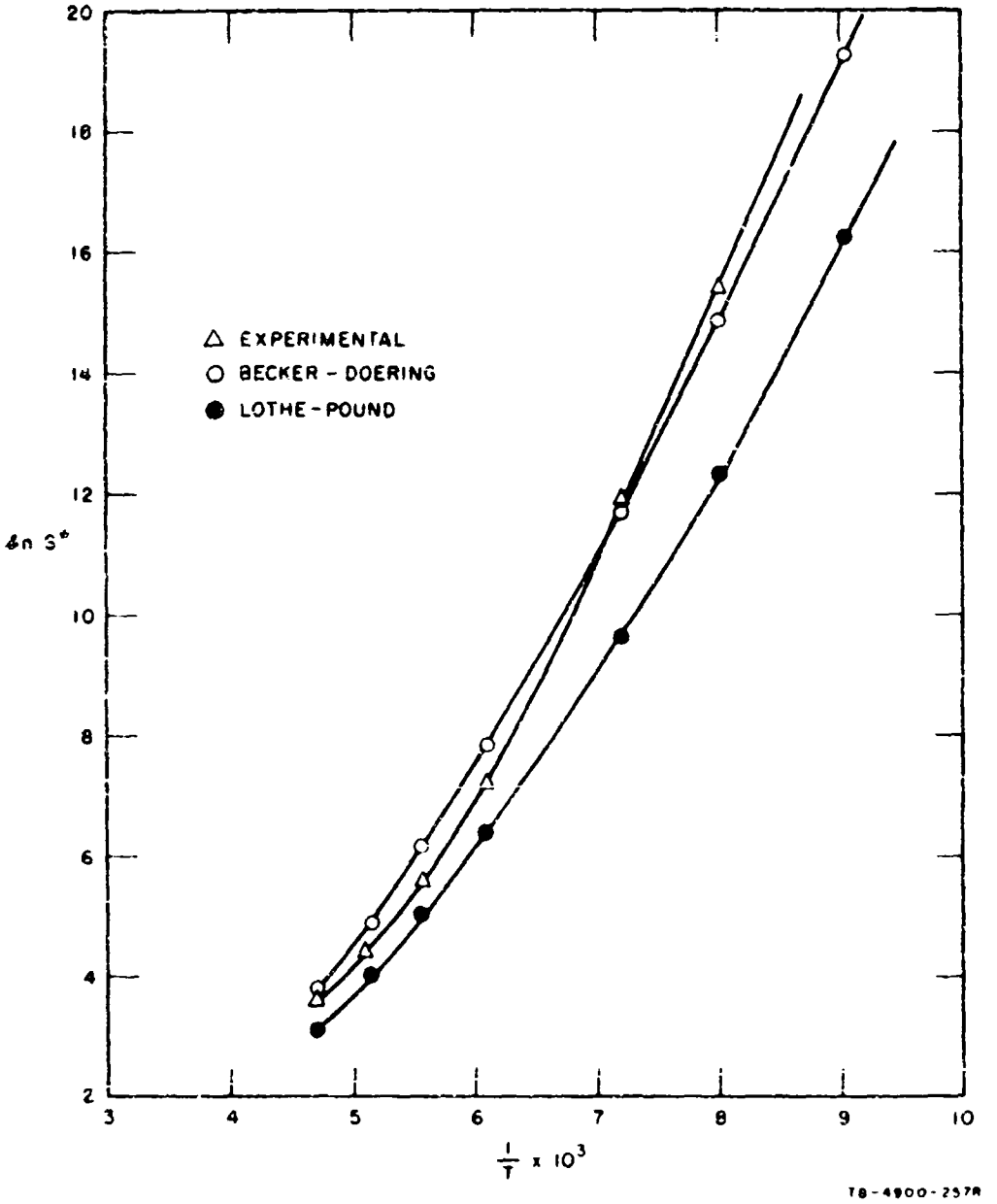

FIG. 10 LOGARITHM OF SUPERSATURATION RATIO AS A FUNCTION OF THE INVERSE OF THE ABSOLUTE TEMPERATURE FOR HOMOGENEOUS NUCLEATION OF CARBON TETRACHLORIDE

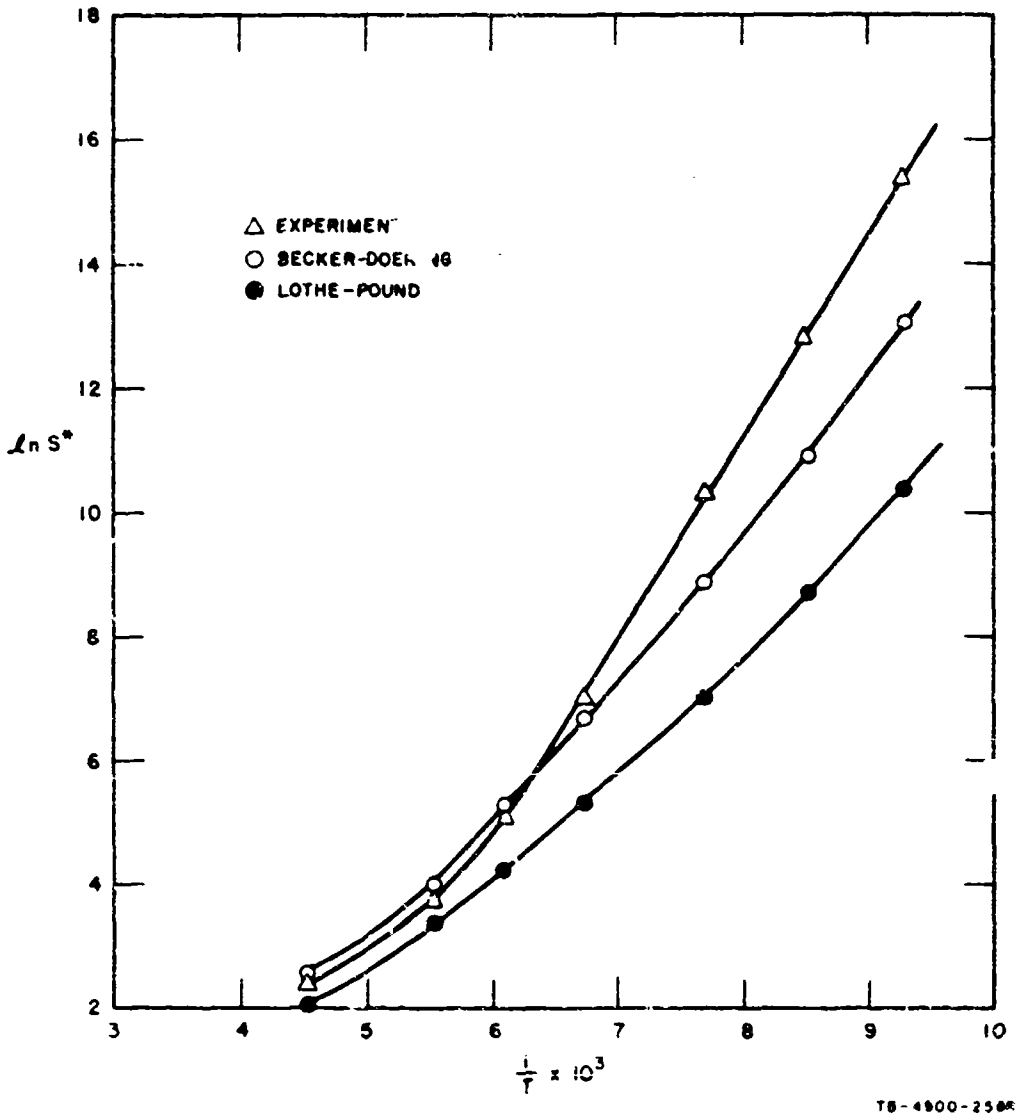

FIG. 11 LOGARITHM OF SUPERSATURATION RATIO AS A FUNCTION OF THE INVERSE OF THE ABSOLUTE TEMPERATURE FOR HOMOGENEOUS NUCLEATION OF CARBON DISULFIDE

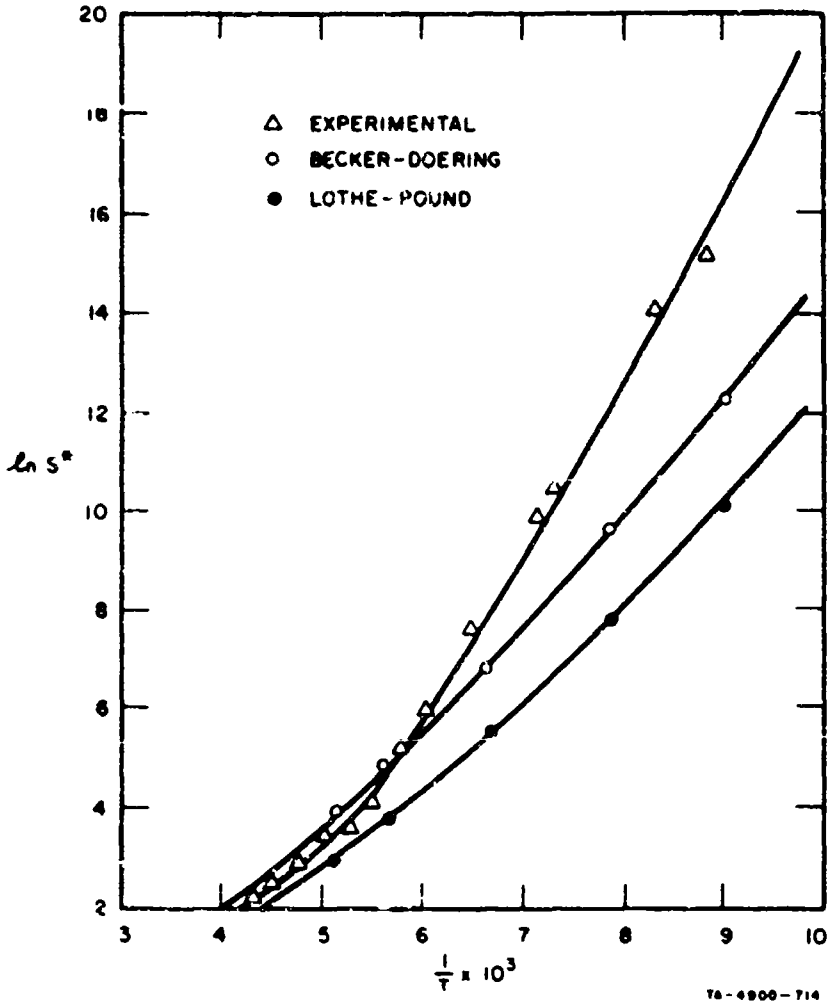

FIG. 12 LOGARITHM OF SUPERSATURATION RATIO AS A FUNCTION OF THE INVERSE OF THE ABSOLUTE TEMPERATURE FOR HOMOGENEOUS NUCLEATION OF CHLOROFORM

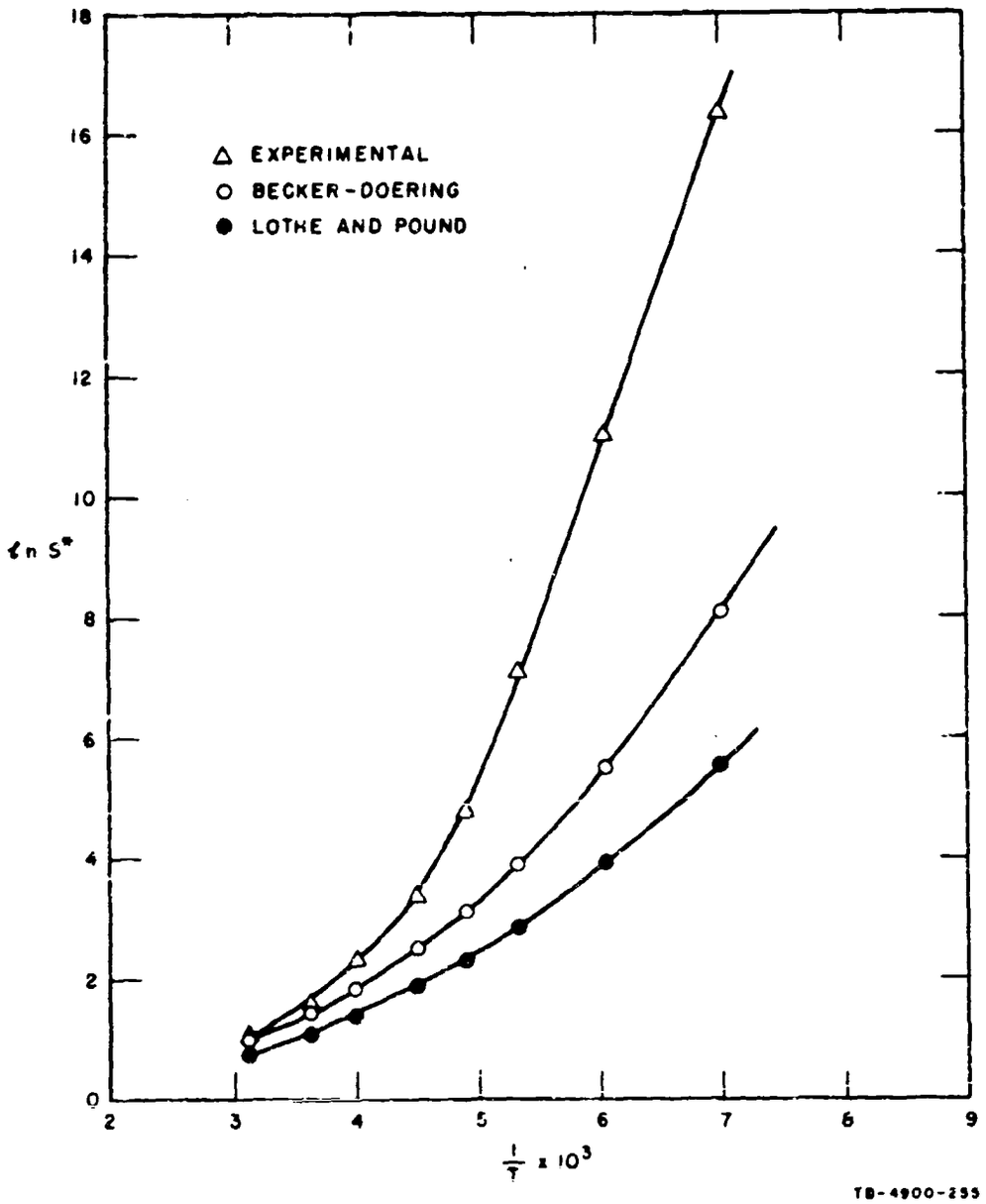

FIG. 13 LOGARITHM OF THE SUPERSATURATION RATIO AS A FUNCTION OF THE INVERSE OF THE ABSOLUTE TEMPERATURE FOR HOMOGENEOUS NUCLEATION OF WATER

the saturated vapor pressure, the surface tension, and the molar entropy at temperature T.

The logarithm of the saturated vapor pressure p_∞ is extrapolated graphically from the linear relationship with $1/T$ (see Appendix). The density is determined by the equation

$$d = \alpha_1 + \alpha_2 t + \alpha_3 t^2 + \alpha_4 t^3 \quad , \tag{38}$$

where t is the temperature in degrees centigrade and α_1, α_2, α_3, and α_4 are experimental constants (see Appendix). For σ at T we use the equation:

$$\sigma = \beta_1 + \beta_2 t + \beta_3 t^2 + \beta_4 t^3 \quad , \tag{39}$$

where β_1, β_2, β_3 and β_4 are constants determined experimentally (see Appendix). The liquid entropy s is computed from

$$s = s^\circ + \int_{298.2}^{T} \frac{C_p}{T}\, dT \quad , \tag{40}$$

where s° is the standard molar entropy for liquid state (at 25°C and atmospheric pressure) and C_p is the molar heat capacity of the liquid at constant pressure.

The physical property data were compiled for the organic compounds and water and then used in the nucleation rate equations of Becker-Doering and Lothe and Pound to obtain the calculated values of $ln\ S^*$, $\mathbf{R}$ and $\mathbf{X}$ (see Figs. 9-13).

$$2(ln\ S^*)^3 + b(ln\ S^*)^2 - a = 0 \quad , \tag{21}$$

$$\mathbf{X}^3 + \mathbf{X}^2 \left\{ b + \lambda - \frac{1}{2} ln\ a - 12\ ln\ \mathbf{X} + \frac{1}{2} ln \left[a + \mathbf{X}^3 + \mathbf{X}^2 (12\ ln\ \mathbf{X} - \lambda) \right] \right\} - a = 0 \quad . \tag{31}$$

A comparison of the theoretical results obtained for $\mathbf{R}$ and $\mathbf{X}$ with the experimental values of $ln\ S^*$ shows a discrepancy between theory and experiment; this discrepancy increases very rapidly as the temperature decreases. Furthermore, the values of S^* become very large at low temperatures and calculated cluster size becomes very small. This discrepancy may be due to the fact that macroscopic properties such as p, d, and σ are assumed to be applicable to very small clusters. The dependence

of the physical properties on cluster size appears to be very important in the case of surface tension.

2. Variation of Surface Tension with Droplet Curvature

The problem of the variation of the surface tension with droplet curvature has been studied very intensively by many investigators, but the relationship between surface tension and curvature has never been resolved. Because of its critical importance in the nucleation model, a study was made of the surface tension of clusters.

We determined indirectly the surface tension (σ_r) as a function of curvature in the following way. We introduced a parameter ρ, defined as the ratio of the surface tension, corrected for the curvature (σ_r) and the bulk value (σ_b). The values of ρ were determined by replacing the theoretical values of S^* in the nucleation rate equation with the measured values. If the Lothe-Pound theory is correct (except for the value of σ), then the function $\rho(i^*) = \sigma_r/\sigma_b$ would allow the theory to predict correctly the value of the critical supersaturation ratio. We thought that use of the experimental values of S^* and of the theory to compute $\rho(i^*)$ might also shed some light on the dependence of surface tension on cluster size.

With ρ thus defined and with a, b, and λ defined by Equations (22), (23), and (30), we obtain

$$\frac{a^r}{a} = \frac{\sigma_r^3}{\sigma^3} = \rho^3 \quad , \tag{41}$$

$$b^r - b = ln\left(\frac{\sigma_r}{\sigma}\right)^{1/2} = \frac{1}{2}\, ln\, \rho \quad , \tag{42}$$

$$\lambda^r - \lambda = 4\, ln\, \frac{a^r}{a} = 12\, ln\, \rho \quad , \tag{43}$$

where a^r, b^r, and λ^r are the values of a, b, and λ for $\sigma = \sigma_r$ or

$$a^r = a\rho^3 \quad , \tag{44}$$

$$b^r = b + \frac{1}{2}\, ln\, \rho \quad , \tag{45}$$

$$\lambda' = \lambda + 12 \ln \rho \quad . \tag{46}$$

Substituting a', b', and λ' from Equations (44)-(46) into (21) [for the Becker-Doering theory] and into (31) [for the Becker-Doering theory corrected for the Lothe and Pound factor] and setting $E = \ln S^*$, we obtain two new equations:

$$a\rho^3 - E^2 \ln \rho - E^2(b + 2E) = 0 \quad , \tag{47}$$

$$a\rho^3 - 11E^2 \ln \rho - \frac{E_n^2}{2} \ln [a\rho^3 - 12E^2 \ln \rho + E^2(E + 12 \ln E - \lambda)]$$
$$- E^2\left(b + E + \lambda - \frac{1}{2} \ln a - 12 \ln E\right) = 0 \quad . \tag{48}$$

Equation (47) yields the values of ρ which we shall use for the correction of the surface tension for small droplets in the case of the Becker-Doering theory; Equation (48) does the same for the Lothe and Pound theory.

Since we wish to determine if the discrepancy between theoretical and experimental values can be ascribed to the use of σ_∞, we also computed the number of molecules i^* in the critical cluster. We examine the function ρ vs i^*.

$$i^* = \frac{2a_i^3}{E^3} \quad . \tag{49}$$

The results of our computation for ρ and i^* are given in Figs. 14-18.

3. Cluster Size and the Surface Tension Correction

In the case of water the function ρ decreases with the size of the droplets and consequently increases with curvature. Dillmann and Sundquist[19] have developed a dangling-bond model for water on the assumption that the effect of curvature on surface-free energy is due to the broken hydrogen bonding of the surface molecules. They calculate a correction of approximately 1.2 for $i^* = 10$ to 110. Our numerically computed results are in qualitative agreement with their calculation, e.g., actually for the point ($S^* = 5.07$, $T = 276.3$K), where ρ is 1.10. However, for the point ($S^* = 6.3 \times 10^4$, $T = 165.24$K), their calculated correction of 1.23 for $i^* = 10$ does not agree with our result of 1.73 for $i^* = 9$.

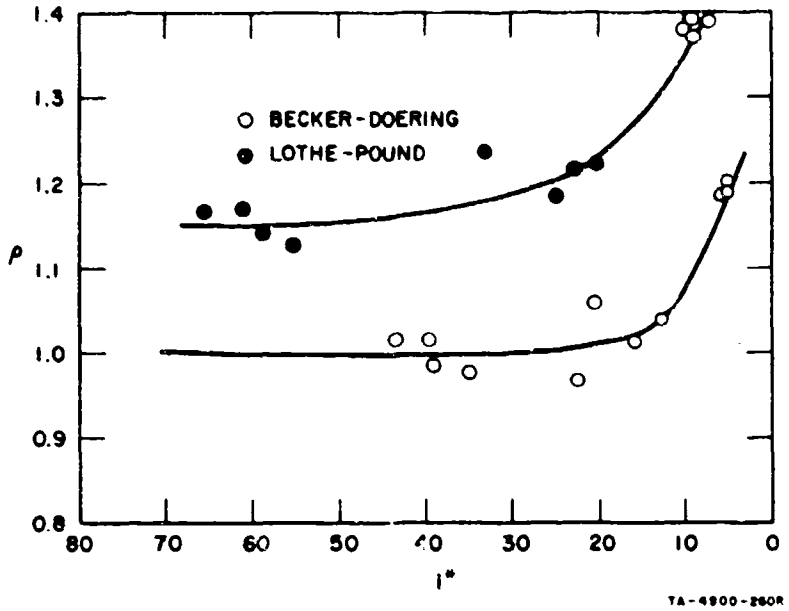

FIG. 14 PARAMETER ρ AS A FUNCTION OF i^* FOR THE SYSTEM, BENZENE + AIR

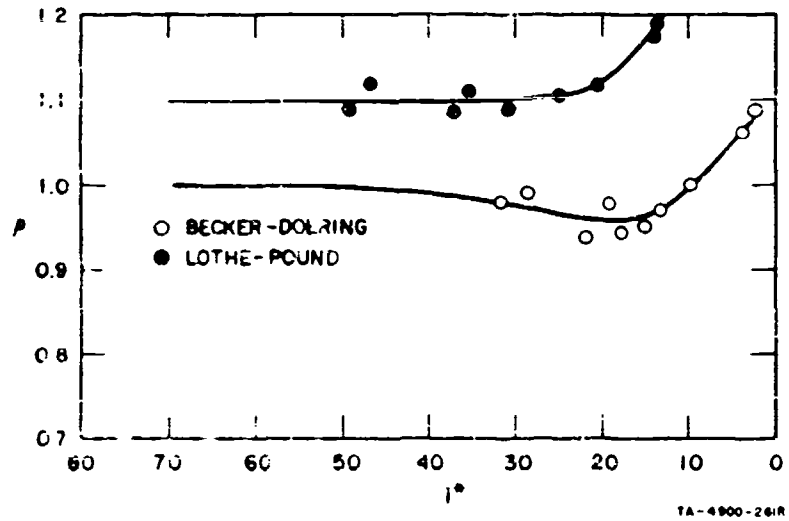

FIG. 15 PARAMETER ρ AS A FUNCTION OF i^* FOR THE SYSTEM, CARBON TETRACHLORIDE + AIR

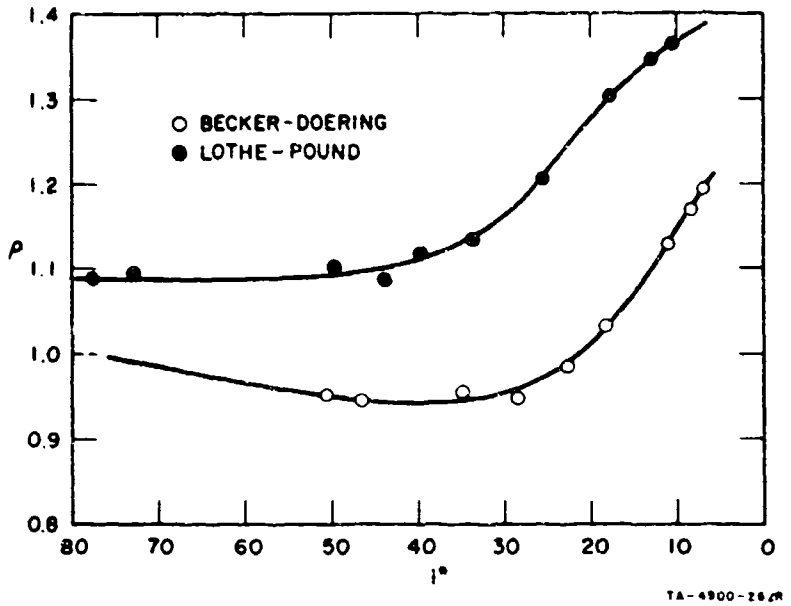

FIG. 16 PARAMETER ρ AS A FUNCTION OF i^* FOR THE SYSTEM, CARBON DISULFIDE + AIR

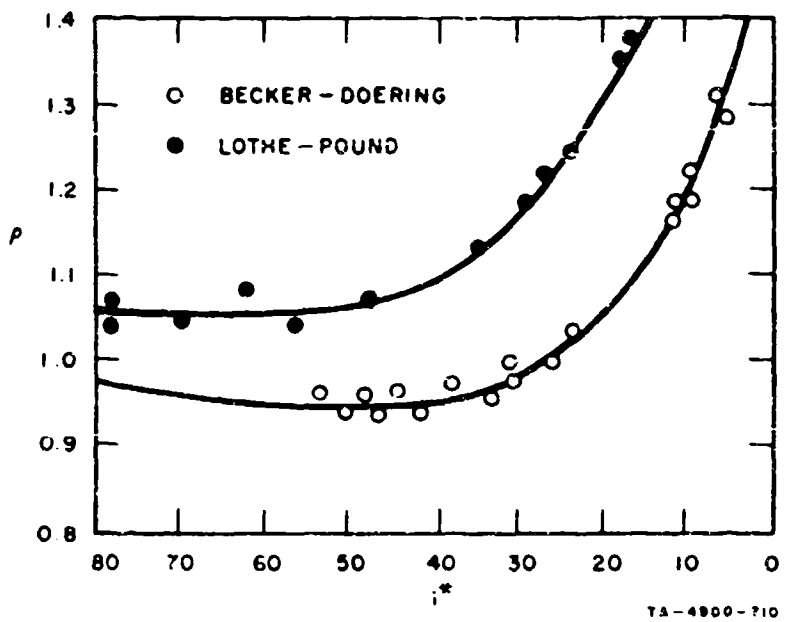

FIG. 17 PARAMETER ρ AS A FUNCTION OF i^* FOR THE SYSTEM, CHLOROFORM + AIR

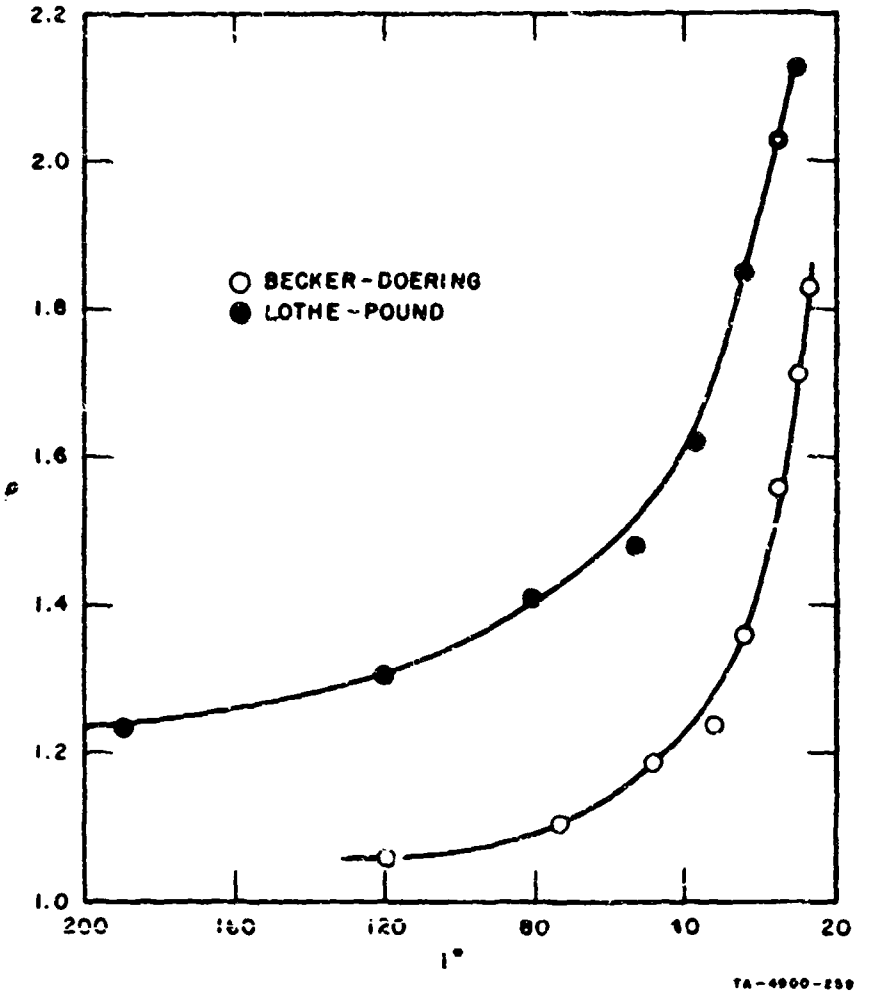

FIG. 18 PARAMETER ρ AS A FUNCTION OF i^* FOR THE SYSTEM, WATER + AIR

In the case of nonpolar molecules (benzene, CCl_4, and CS_2), we find that ρ does not increase with curvature and that ρ is approximately constant when the size of the nuclei is large enough; but for a smaller size nuclei, ρ increases markedly with curvature. In the case of $CHCl_3$, for large size values of i^*, Chloroform is a slightly polar compound and its $\rho - i^*$ curve resembles the non-polar case except at low temperature (small i^*), where the effect of polar forces may be evident.

It is to be expected that surface free energy for small drops should increase with any orientationed force field and specifically with dipole moment. In the case of benzene we may have an orientational effect tha

increases ρ with curvature. Benzene is a flat molecule, and it should be more difficult to get the surface molecules in their oriented positions and therefore a geometrical hindrance effect will strongly increase ρ. This will explain why, although the benzene has no electric dipole moment, ρ increases rapidly for small values of ε^*, as in the case of polar molecules.

LITERATURE CITED

1. Fuks, N. A., The Mechanics of Aerosols, Moscow Acad. Sci. USSR, Inst. Sci. Inf., transl. from Russian for MSP by E. Lackowiz, CWL-Spec. Publ. 4-12, 339 (1955).

2. Gibbs, J. W., *Collected Works*, Vol. I, Thermodynamics, Yale University Press, New Haven (1948).

3. Volmer, M., and Weber, A., Z. Phys. Chem. 119, 277 (1926).

4. Becker, R., and Doering, W., Ann. Phys. 24, 719 (1935).

5. Poppoff, I. G., Research studies on the dissemination of solid and liquid agents, Stanford Research Institute Ninth Quarterly Progress Report on Contract No. DA-18-035-AMC-122(A), April 1 to June 30 (1965).

6. Lothe, J., and Pound, G. M., J. Chem. Phys. 36, 2080 (1962).

7. Feder, J., Hirth, J. P., Lothe, J., Russell, K. C., and Pound, G. M., Heterogeneous combustion in *Progress in Astronautics and Aeronautics*, 15. p. 670, Academic Press, New York and London (1964).

8. Wilson, C. T. R., Phil Trans. Roy. Soc. (London) 192, 403 (1899), 193, 289 (1899); Phil. Mag. 7, 681 (1904); Trans. Roy. Soc. (London) A189, 265 (1897); Powell, C. F., Proc. Roy. Soc. (London) A119, 553 (1928).

9. Volmer, M., and Flood, H., Z. Phys. Chem. A170, 273 (1934).

10. Clarke, J. V., and Rodebush, W. H., Nucleation in supersaturated vapors, Ph.D. Thesis of J. V. Clarke, University of Illinois, Urbana (1952).

11. Katz, J. L., and Ostermier, B. J., A diffusion cloud chamber investigation of homogeneous nucleation (preprint), North American Aviation Science Center, Thousand Oaks, Calif. (1966).

12. Higuchi, W. I., and O'Konski, C. T., J. Colloid. Sci. 15, 14 (1960).

13. Bodenstein, M., and Wolgast, K., Z Phys. Chem. 61, 422 (1908).

14. Langmuir, I., J. Am. Chem. Soc. 30, 1742 (1908).

15. Benton, A. F., J. Am. Chem. Soc. 53, 2984 (1931).

16. Hirth, J. P., and Pound, G. M., *Progress in Materials Science*, Condensation and Evaporation, Vol. 11, Macmillan and Co., Ltd., New York (1963).

17. Sander, A., and Damkochler, G., Naturwissen 31, 460 (1943).

18. Madonna, L. A., Sciulli, C. M., Canjar, L. N., and Pound, G. M., Proc. Phys. Soc. (London) 78, 1218 (1951).

19. Oriani, R. A., and Sundquist, B. E., J. Chem. Phys. 38, 2082 (1965).

20. *International Critical Tables of Numerical Data, Physics, Chemistry, and Technology*, Natl. Res. Council, (a) 3, 28; (b) 4, 447-448, McGraw-Hill Book Company, Inc., New York, Toronto and London (1933).

21. Timmermans, J., *Physico-Chemical Constants of Pure Organic Compounds*, Elsevier, Amsterdam, London, and New York, *Vol. I* (1950); *Vol. II* (1965).

22. Hodgman, C. D., *Handbook of Chemistry and Physics*, Chemical Rubber Co., Cleveland (1947).

23. Stull, D. R., J. Am. Chem. Soc. 59, 2726 (1937).

24. Oliver, G. D., Eaton, M., and Huffman, H. M., J. Am. Chem. Soc. 70, 1502 (1948).

25. Brown, O. L. I., and Manor, G. G., J. Am. Chem. Soc. 59, 500 (1937).

26. *Selected Values of Physical and Thermodynamic Properties of Hydrocarbons and Related Compounds*, API Research Project 44, Carnegie Press, Pittsburgh (1953).

27. McDonald., J. E., J. Geophys. Res. 70, 1553 (1965).

GLOSSARY

A	A nucleus or particle
A_i^*	Critical nucleus containing i molecules
α_c	Condensation coefficient
$C_{p(v)}$	Average heat capacity at constant pressure (cal/mole) of vapor
C_p	Average heat capacity at constant pressure
C_V	Average heat capacity at constant volume
d	Density (g/cc)
F_c	Cold stream flow rate (ml/min)
F_w	Warm stream flow rate
Γ	Lothe-Pound correction factor
ΔG	Free energy of formation of droplet (per mole)
ΔG°	Free energy of formation
ΔG^*	Free energy change of formation of critical nucleus
$\Delta G_2^{*\prime}$	Free energy change of rotation of critical nucleus
ΔG_1°	Free energy of formation (per drop)
$\Delta G^{*\prime}$	Free energy change accompanying rotational and translational degrees of freedom in critical nucleus
$\Delta G_1^{*\prime}$	Free energy change of translations of critical nucleus
$\hbar$	Planck constant divided by 2π
i^*	Number of molecules in critical nuclei
I	Moment of inertia
J	Nucleation rate
k	Boltzmann's constant
K	Coagulation coefficient
m	Molecular mass
M	Molecular weight
n	Number of molecules/cc

n^*	Concentration of critical nuclei
n_i^*	Concentration of nuclei containing i molecules
n_1	Number of molecules/cm^3
N	Avagadro's number
ω	Frequency of collision of nuclei per surface unit
p	Vapor pressure (mm Hg)
p_∞	Saturated vapor pressure (mm Hg)
ΔQ_c	Total heat gain of cold stream
ΔQ_w	Total heat loss of warm stream
r	Radius
r^*	Radius of critical nucleus
R	Gas constant (Boltzmann constant × Avagadro's number)
ρ	Ratio of surface tensions σ_b/σ_r
s	Molecular entropy
S	Supersaturation ratio
S^*	Critical supersaturation ratio
s°	Standard molecular entropy
σ	Surface tension (dynes/cm)
σ_r	Surface tension of drop of radius r
σ_b	Bulk surface tension
$\sigma_{A,B}$	Collision cross section (diameter of particles A and B)
T	Absolute temperature
T_i	Initial temperature
T_F	Terminal temperature
t	Temperature (°C)
V_0	Molar volume
Z	Nonequilibrium factor
Z_{AB}	Number of collisions/sec between A and B particles

APPENDIX

PHYSICAL PROPERTIES USED IN NUCLEATION CALCULATIONS

Density (d) Relative to Water at 4°C

Water:[20(b)] $d = 0.9994 + 1.896 \times 10^{-4}(t + 4) - 1.0417 \times 10^{-5}(t + 4)^2 - 6.95 \times 10^{-8}(t + 4)^3$

CCl_4:[21] $d = 1.63255 - 1.911 \times 10^{-3}\, t - 0.690 \times 10^{-6}\, t^2$

Benzene:[21] $d = 0.90005 - 1.0636 \times 10^{-3}\, t - 0.0376 \times 10^{-6}\, t^2$

CS_2:[21] $d = 1.29272 - 1.481 \times 10^{-3}\, t - 3.06 \times 10^{-7}\, t^2$

$CHCl_3$:[20,21] $d = 1.52643 - 1.8563 \times 10^{-3}\, t - 0.5309 \times 10^{-6}\, t^2 - 8.81 \times 10^{-9}\, t^3$

where t is the temperature in degrees centigrade

Surface Tension (σ) in dynes/cm

Water:[20] $\sigma = 76.96 - 0\ 152(t + 8) + 0.7882 \times 10^{-4}(t + 8)^2 - 2.56 \times 10^{-6}(t + 8)^3$

CCl_4:[20,21] $\sigma = 29.38 - 0.13975\, T + 3.875 \times 10^{-4} t^2$

Benzene:[20,21] $\sigma = 31.58 - 0.137\, t + 0.0001\, t^2$

CS_2:[20,21] $\sigma = 35.28 - 0.15217\, t + 0.8333 \times 10^{-4}\, t^2$

$CHCl_3$:[20,21] $\sigma = 28.6 - 0.1363(t - 10)$

Liquid Heat Capacity C_p at Constant Pressure in cal/mole

Water:[22] $C_p = 218.765 - 2.0182\, T + 6.769 \times 10^{-3}\, T^2 - 7.575 \times 10^{-6}\, T^3$

CCl_4:[23] $C_p = 219.18 - 2.2173\, T + 8.5583 \times 10^{-3}\, T^2 - 1.0833 \times 10^{-5}\, T^3$

Benzene:[24] $C_p = -37.816 + 0.6104\, T - 1.8938 \times 10^{-3}\, T^2 + 2.140 \times 10^{-6}\, T^3$

CS_2:[25] $C_p = 17.825 + 7.6 \times 10^{-4}\, T$

$CHCl_3$:[21,26] $C_p = 12.4822 + 0.05137\, T$

Standard Entropy ($s°$) (at 25°C/atm of pressure in cal. per mole and per degree)

Water: $s° = 16.73$

CCl_4:[23,26] $s° = 51.25$

Benzene:[24] $s° = 41.30$

CS_2:[25] $s° = 36.10$

$CHCl_3$:[26] $s° = 48.5$

Unclassified
Security Classification

DOCUMENT CONTROL DATA - R & D

(Security classification of title, body of abstract and indexing annotation must be entered when the overall report is classified)

1. ORIGINATING ACTIVITY (Corporate author)	2a. REPORT SECURITY CLASSIFICATION
Stanford Research Institute Menlo Park, California 94025	Unclassified
	2b. GROUP N/A

3. REPORT TITLE

CONDENSATION STUDIES

4. DESCRIPTIVE NOTES *(Type of report and inclusive dates)*

Special Technical Report No. 10

5. AUTHOR(S) *(First name, middle initial, last name)*

Robbins, R. C. and Naar, C.

6. REPORT DATE	7a. TOTAL NO. OF PAGES	7b. NO. OF REFS
April 1967	58	27

8a. CONTRACT OR GRANT NO.	9a. ORIGINATOR'S REPORT NUMBER(S)
DA-18-035-AMC-122(A) b. PROJECT NO.	SPEC-TR-10, PAU-4900
c. Task 1B522301A08101 d.	9b. OTHER REPORT NO(S) *(Any other numbers that may be assigned this report)* N/A

10. DISTRIBUTION STATEMENT This document is subject to special export controls and each transmittal to a foreign government or foreign nationals may be made only with prior approval of the CO, Edgewood Arsenal, Attn: SMUEA-TSTI-T, Edgewood Arsenal, Maryland 21010.

11. SUPPLEMENTARY NOTES	12. SPONSORING MILITARY ACTIVITY
Dissemination investigations of liquid and solid agents	CO, Edgewood Arsenal Research Laboratories Edgewood Arsenal, Maryland 21010

13. ABSTRACT

(U) Condensation processes are important in the thermal dissemination of CW agents. Heterogeneous and homogeneous nucleation was studied to determine the important factors controlling condensing systems.

Effects of salt nuclei on the particle size distribution of the disseminated aerosol were studied and special pyrotechnic systems which were salt nuclei-free were investigated.

Aerosols composed of two- to five-micron-diameter particles with a high degree of particle size homogeneity make the optimum aerosol for lung retention and maximum transparency. The production of such an aerosol was shown to be feasible by the technique of incorporating nonvolatile "giant nuclei" material in the pyrotechnic mix. These giant nuclei when disseminated with the agent vapor acted as preferential condensation sites and as small particle scavengers by coagulation. The secondary process of coagulation was shown to be important in removing the highly visible submicron particles. A pyrotechnic dissemination system was suggested to produce uniform, low visibility aerosols which included coagulation of the small particles to be disseminated on giant nuclei at elevated temperature and high concentrations.

(over)

14 KEY WORDS	LINK A		LINK B		LINK C	
	ROLE	WT	ROLE	WT	ROLE	WT
Condensation						
Thermal dissemination						
Pyrotechnic						
Nucleation						
Particle size distribution						
Aerosols						
Coagulation						
Chemical agent						

Homogeneous nucleation always occurs in condensing systems of high vapor concentrations even in the presence of foreign nuclei. Critical supersaturation ratios of a number of compounds were measured by a newly developed experimental method. It was demonstrated that the classical Becker-Doering theory is inadequate for the preparation of nucleation models. A modified model is presented showing the interrelationships among physical properties, chemical structure, and temperature.